ELSEVIER

Contents lists available at ScienceDirect

Applied Energy

journal homepage: www.elsevier.com/locate/apenergy



Characterization by key performance indicators of SFERA-III project to ALTAYR packed-bed prototype

Esther Rojas ^{a,*}, Elisa Alonso ^b, Margarita Rodríguez-García ^c, Rocío Bayón ^a, Antonio Avila-Marín ^a

- ^a CIEMAT-PSA, Avda. Complutense, 40, 28040 Madrid, Spain
- b ETSII-Universidad Politécnica de Madrid, c/José Gutiérrez Abascal, 2, 28006 Madrid, Spain
- ^c CIEMAT-PSA, Carretera de Senés, km 4, 04200 Tabernas (Almería), Spain

HIGHLIGHTS

- Analyse standardization activities related to thermal energy storage prototypes
- • Testing of sensible and latent thermal energy storage prototypes
- • Key performance indicators applied to a packed-bed prototype

ARTICLE INFO

Keywords: Thermal energy storage Prototypes Testing KPIs Guidelines Packed-bed

ABSTRACT

The objective of this study is to assess the viability of implementing the methodology proposed in the SFERA-III project for the assessment of key performance indicators (KPIs) of thermal storage prototypes in a specific packed-bed device. SFERA-III project is an EU funded project aiming, among others, to upgrade the infrastructures and services related to Concentrating Solar Thermal technologies. In order to improve the quality of services in relation to the testing of thermal energy storage prototypes, a protocol and KPIs were defined and validated with different types of devices, though none of them was a packed-bed. This study elucidates the challenges encountered in the implementation of the protocol on a packed-bed prototype, alongside the proposed alternative solutions and their influence on the resulting KPIs. The analysis demonstrates that the SFERA-III Key Performance Indicators are an appropriate means of evaluating packed bed thermal energy storage prototypes. Consequently, the use of these KPIs as a standard is supported.

1. Introduction

Energy storage is currently considered a key piece to achieve a sustainable, secure and decarbonized energy system. Climate and energy policies worldwide agree on achieving ambitious targets for energy savings and renewables to be included in the energy market. These targets cannot be achieved without an appropriate management of the renewable energy production and of the energy fluxes in both industry and building sectors. Energy storage, wider interconnections, and smart grids can provide the flexibility that the energy system based on renewables requires [1].

Energy storage systems allow energy consumption to be decoupled in time from its production, whether it be electrical energy or thermal energy. The advantages offered by thermal energy storage (TES) technologies are well known in the building sector for heating and cooling, where hot-water tanks, with more or less sophisticated designs, are used. On the contrary, these benefits are quite unknown to the industrial and power generation sectors, although, in the power sector, there are already commercial TES systems of very large storage capacity used in concentrating solar thermal power (CSTP) plants. Examples of these power plants are Noor II and Noor III that have 200 MW_e / 1200 MW_e (i.e. 6 h working at nominal power without solar input) and 150 MW_e / 125 MWh_e (i.e. 7,5 h at nearly nominal power), respectively [2,3] or Atlántica Solana Generating Station, in Arizona, with 250 MW_e /1500 MWh_e (i.e. 6 h at nearly nominal power [4]). The current average investment cost for CSTP-TES systems is around 40 ℓ / kWh_e [5].

To stand out the competitiveness of TES, an interesting exercise is to

E-mail address: esther.rojas@ciemat.es (E. Rojas).

 $^{^{\}ast}$ Corresponding author.

Nomencl	ature	out	at the outlet
		pb	related to packed-bed
\boldsymbol{A}	Area (m ²)	rated	rated value
CF	Comparison Factor (–)	RB	related to refractory bricks
c_p	Heat capacity (J/K·kg)	SE	related to steel envelope
E	Energy (J)	SS	related to steady-state conditions
h	Heat loss coefficient (W/m ² K)	TES	related to Thermal Energy Storage
m	Mass (kg)	411	
ṁ	Mass flow (kg/h)	Abbreviat	
P	Thermal Power (kW)	ANSI	American National Standards Institute
\mathcal{S}	Stratification Index (–)	ASHRAE	American Society of Heating, Refrigerating and Air-
SC	Storage Capacity (kWh or J)		Conditioning Engineers
T	Temperature (°C)	CSTP	Concentrating Solar Thermal Power
t	Time (s)	ECES	Energy Conservation through Energy Storage
TSC	Theoretical Storage Capacity (Capacitance) (kWh or J)	EU	European Union
UR	Utilization Rate (–)	HTF	Heat Transfer Fluid
		IEA	International Energy Agency
Symbols		IEC	International Electrotechnical Commission
η	(Energy) Efficiency (–)	IRENA	International Renewable Energy Agency
${\it \Xi}$	Exergy (J)	JRA	Joint Research Activity
Ψ	Exergy Efficiency (–)	KPI	Key Performance Indicator
C . 1		PBTES	Packed-Bed Thermal Energy Storage
Subscripts		PCM	Phase Change Material
	related to ALTAYR facility	PV	PhotoVoltaic
	related to ambient	SFERA	Solar Facilities for the European Research Area
	related to charge	SHC	Solar Heating and Cooling
	related to discharge	SOC	State Of Charge
J	related to filler	SolarPAC	CES Solar Power And Chemical Energy Systems
	related to the heat transfer fluid	STE	Solar Thermal Energy
IF	related to insulating fibber	TCP	Technology Collaboration Programme
in	at the inlet	TES	Thermal Energy Storage
level1	at level 1	TS	Technical Specification
level9	at level 9	UNE	Una Norma Española (Spanish National Standardization
	related to thermal losses		Body)
max	maximum	WG	Working Group
mean	mean value	WOS	Web Of Science
min	minimum		

compare CSTP and Photovoltaic (PV) from a purely economic point of view. Although in principle, PV holds a significantly superior position, the results reverse when considering in the analysis the inclusion of energy storage, thermal for CSTP and electrical for PV [6]. These two facts -large storage capacity and low cost- place TES systems in a privileged -but, unfortunately, untapped- position in the topic of storing energy for power plants. This is the reason why the use of these TES systems to store large amounts of energy from wind and PV is currently being considered and explored, not only by research centres but also by renewable companies [7]. As an example, Siemens-Gamesa, a wind power company, developed what they call its electrothermal energy storage system, which uses volcanic rocks to store thermal energy provided by hot air heated by electric heaters. They erected in 2019 in Hamburg, Germany, a demonstrator for this concept that was able to store up to 130 MWh thermal energy [8], and tested it until May 2022 [9,10]. In the industrial sector, it is being recognized that TES can significantly support the decarbonisation of industrial heating and cooling while increasing the flexibility and security of the energy system [11]. According to IRENA [7], the specific features of TES, such as seasonal capability, large storage capacity, high round trip efficiency and long-life cycles, will triple by 2030 the installed capacity at the end of 2019, reaching at least 800 GWh.

Previous target will not be achieved without appropriate measures for technological development and innovation. Great efforts to advance in such a technological development can be seen when looking at the number of articles listed in the Web of Science Core Collection for the last 10 years. As displayed in Fig. 1a, this number has doubled from 2015 to 2022 and mainly under the category of Energy Fuels (see Fig. 1b). Moreover, between 1 % and 2 % of those articles each year are devoted to the evaluation of thermal energy storage prototypes. The innovations included in these prototypes, which are used to store energy, as sensible, latent or thermochemical energy, are difficult to compare since there are no standardized figures of merit or key performance indicators (KPIs) that are accepted by the scientific community, both for electricity generation and for industrial process heat above 180 $^{\circ}$ C.

Firstly, this article presents and arranges the main standards, test guidelines and the latest published articles on KPIs used in prototype thermal energy storage in sensible heat or latent heat. Secondly, the article applies the most recent and updated guidelines, proposed in SFERA-III project, to evaluate the KPIs in a specific TES packed-bed device, providing new insights and reinforcing the need for continued standardization efforts in the field of TES. With this aim, the article is structured as follows: section 2 summarizes the main standards, guidelines and recent literature works about TES prototypes, section 3 describes the packed-bed used for the experimental tests of this work, section 4 describes the charging and discharging matrix of tests, section 5 used the KPIs adopted in the SFERA-III project to finally presents the conclusions in section 6.

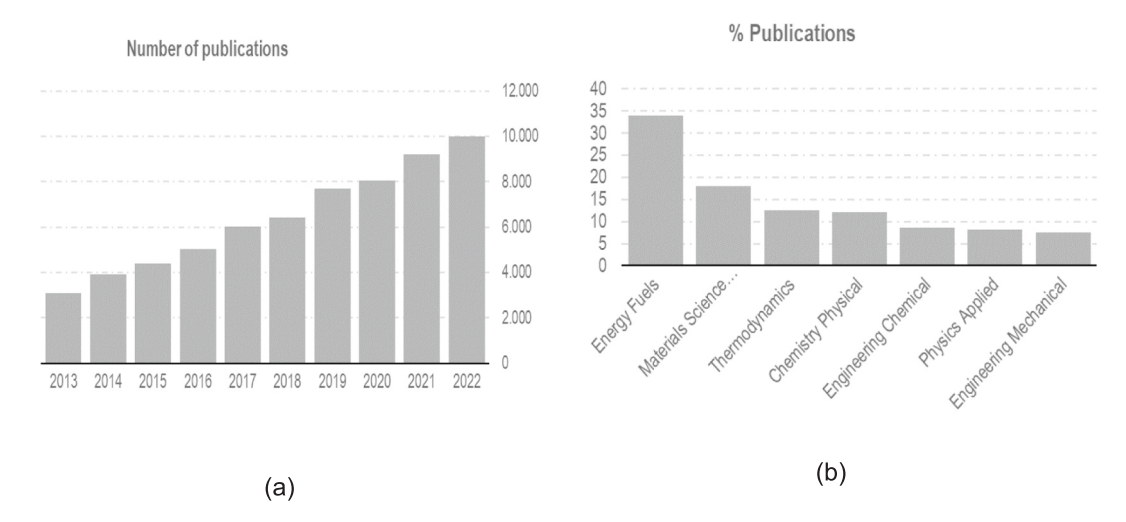


Fig. 1. (a) Number of publications per year and (b) percentage of those according to Web of Science Categories, since 2013 until 2022, on "Thermal Storage", in the WOS Core Collection (updated in December 2023).

2. Metrics used in thermal energy storage prototypes

Despite the growing interest in TES systems, there remains a significant lack of standardized procedures for evaluating their performance, as detailed in the following subsections. The absence of universally accepted key performance indicators (KPIs) has resulted in fragmented and incomparable results between different studies, limiting the ability to efficiently advance TES technologies. The next subsections present, first, the main standardization activities and test guidelines used for TES, second, the main figures of merit used in the most recent research works on TES prototypes, and finally, a summary and objectives of this research.

2.1. Standardization activities

Since the 1980s, various working groups have been working to establish standardized performance indicators for different storage systems, such as sensible and latent heat thermal energy storage devices used in heating, air-conditioning and domestic hot water systems. More recently, within the framework of the International Energy Agency (IEA) and some EU-funded projects, new efforts have been made in order to achieve standards for sensible or latent heat TES for power generation at medium to high temperatures. This section briefly summarizes the main achievements.

The ANSI/ASHRAE standards 94.3-2010 ("Methods of Testing Active Sensible Thermal Energy Devices Based on Thermal Performance" [12]) and 94.1-2010 ("Methods of Testing Active Latent -Heat Storage Devices Based on Thermal Performance" [13]) address the determination of the thermal performance of sensible and latent heat energy storage devices, respectively, but for their use in heating, air conditioning and service hot water systems. Apart from having several typos and not being specifically intended for prototypes, some researchers encountered problems in applying these standards to the thermal storage prototypes they were developing. For example, the ANSI/ASHRAE 94.3-2010 standards require pre-testing of a uniform initial temperature inside the device. The 'uniform temperature' is defined based on a dimensionless residual energy which must be less than 0,005, which can be difficult to achieve in prototypes mainly due to the relatively large amount of thermal losses. To have the initial temperature as uniform as possible, some prototypes [14,15] add electric heaters around the TES tank.

In the context of the EU funded SFERA project (GA. 228,296) [16], an initial endeavour was undertaken to construct specific prototype protocols for sensible or latent thermal energy storage prototypes

intended for applications in power generation and medium-high temperature industrial processes. The deliverable 15.2 "Definition of standardised procedures for testing thermal storage prototypes for concentrating solar thermal plants" [17], dealt with the specific features of working at higher temperature than in water storage devices. Although based on the experience of the participants, all the work done on this deliverable was paperwork, which unfortunately resulted in unclear descriptions of some concepts.

After the completion of SFERA project, the activity on defining test protocols for thermal storage prototypes continued, among others, through the Thermal Energy Storage Working Group (TES WG) of the SolarPACES TCP [18], which published in 2016 a report entitled "Definition of common procedures for testing thermal storage prototypes for STE plants", where the problems related to not having a uniform initial temperature in the device when charge/discharge were faced. Nevertheless, since this activity was not funded, no great progress was made apart from highlighting the necessity of including this research in a future funded project. Deliverable 15.2 of SFERA project and the report of the TES WG were quite useful for the Spanish standard UNE 206012:2017 "Caracterización del sistema de almacenamiento térmico para aplicaciones de concentración solar con captadores cilindroparabólicos" [19], and the international specification IEC TS 62862-2-1:2021 "Solar thermal electric plant - Part 2-1: Thermal energy storage systems -characterization of active, sensible systems for direct and indirect configurations" [20]. These standards deal with thermal storage systems at power plant level, which implies a much larger size than prototypes and certain limitations for testing -the energy source is a solar field-. These characteristics and limitations had to be considered when defining the test protocols.

IEA-ECES Annex 30 was also aware of the lack of an adequate terminology to characterize TES prototypes and proposed the definitions—but not any testing procedure to obtain them—for seven technical parameters or KPIs [21]: Nominal Power—based on a discharging process-; Response Time—as the time required when initializing discharge to achieve the nominal/design power-; Efficiency—as the ratio of heat absorbed by the Heat Transfer Fluid (HTF) in discharge to the energy absorbed by the TES device during charge-; Auxiliary Energy Ratio—as the ratio of the energy consumed by all the components of the system during the standby, charging, storage and discharging phases (full cycle of the TES system) to the heat delivered during discharge-; Energy Storage Capacity—as the total amount of heat that can be absorbed during charge under nominal conditions (it is what the Theoretical Storage Capacitance—/Capacity is defined in ANSI 94.3—2010 and SFERA-III protocols); Minimum Cycle Length—or shortest period of time required for completely

charge and discharge the system at nominal conditions-; and Partial Load Suitability -as a qualitative indicator that denotes the suitability of a TES system to work under partial load operating conditions-. Since no test procedures were proposed to derive these KPIs, there is some uncertainty on what they refer to. For example, it is not clear whether the nominal power figure should be derived from the temperatures of the HTF or from the ones of the storage material.

In the EU funded SFERA-III project, under the Joint Research Activity (JRA) "Development of test procedures for materials and components of thermal storage systems" [22], a task was devoted to providing definitions of figures of merit and guidelines to quantify them for TES prototypes for power and/or industrial applications, i.e., at temperatures above 100 °C. The KPIs proposed and the specific procedures for their estimation in a systematic and reproducible way are Storage Capacity, Utilization Rate, Mean Thermal Power -associated to the discharging time-, Thermal Losses, Storage Efficiency, Storage Exergy Efficiency, and Auxiliary Power Consumption. The guideline proposed in the project is available in the public deliverable D6.3, "Protocol for testing sensible and latent storage prototypes. Towards the Standardization of testing prototypes for storage systems" [23]. The thermal storage technologies considered are single media thermocline tank (with molten salts or thermal oil as HTF), concrete storage modules, dual media thermocline tank (with molten salts or thermal oil or air as HTF; and rocks, sand, or slags as filler material), solid particles tank in fluidized bed and latent heat storage with Phase Change Material (PCM) in a shell-and-tubes design. The guideline has been verified using experimental data of four case studies: a finned tube and shell latent storage [24], a concrete regenerator [25], a molten solar salt thermocline [26] and a particle storage tank, [23].

Table 1 and Table 2 show the comparison of the KPIs of the main

charging process

flow, to the device during a

standards and guidelines currently available: ANSI/ASHRAE 94.3-2010, ANSI/ASHRAE 94.1-2010, SFERA and SFERA-III.

2.2. Test procedures for TES prototypes

The lack of agreement in testing thermal storage prototypes has made that each group of researchers uses its own figures of merit or KPIs, which prevents a proper comparison between different solutions for a similar application. Reviewing the figures of merit of all tested thermal storage prototypes available in the literature would take around an entire book to finally conclude that the definitions of the KPIs can be very different in each case. Therefore, this section mentions some of the most recent articles on thermal storage prototype testing as examples of the variety of definitions and KPIs used. The reviewed literature is organized according to the typology of the TES device tested (latent heat and sensible heat).

2.2.1. Characterization of latent heat prototypes

Latent heat prototypes are those that store heat at a nearly constant temperature while some fluid or solid material changes its phase. The followings are the most recent works dealing with this concept.

Li et al. [27] proposed a TES Rate Density already defined by Xu and He [28], to evaluate the thermal performance of a two-layered high temperature packed-bed TES (PBTES) with changed-diameter macro encapsulated PCM filler. It is an index related to what they called TES Charging Rate (ratio between the heat energy provided by the HTF in a charging process and charging time) and the mass of the filler -in this case the PCM and the encapsulation masses-. The HTF used was air heated up to 450 °C in charge. It was assumed that the charging process ended when the temperature of the PCM in the locations close to the

Table 1 KPIs of the different standards and guidelines currently available. 1 It is not considered as a KPI but it is mentioned; 2 Highlighting the influence of the initial conditions on the obtained value for this parameter; ³ This is a 1st Law Thermodynamic approach.

ANSI/ ASHRAE 94.3–2010 (Sensible) ANSI/ ASHRAE 94.1–2010 (Latent)	Charge capacity: heat transferred to the device, which is at an initial temperature, by a HTF at a certain temperature and mass flow, during a period of time
SFERA	
SFERA-III	Charge capacity ¹ : heat transferred by the HTF, which is at a certain temperature and mass

Discharge capacity: heat transferred from the device, which is at an initial temperature, to a HTF at a certain temperature and mass flow, during a period of time

Thermal capacity or storage capacity: heat transferred from the device, which is at an initial temperature, to the HTF at a certain inlet temperature and mass flow, in a full discharge. Related to Half capacity cycles: number of consecutive cycles (charge&discharge), under nominal conditions, to reduce the storage capacity to half the design capacity

(that under nominal conditions and

from a full charged device)

Thermal capacity or storage capacity2: heat transferred from the device, which is at an initial temperature, to the HTF at a certain inlet temperature and mass flow, in a full discharge. Rated Storage Capacity, if the device works under rated mass flow conditions

Charge test time: duration of single transient test adding energy to the device

Charging time between 2 different storage levels: duration of single transient test adding energy to the device between 2 storage levels.

- If the HTF flows in nominal conditions → Nominal charging time
- · If, in addition, it works between minimum and maximum storage levels → Characteristics nominal charging time

Charging time^{1,2}: duration of single transient test adding energy to the device between 2 storage levels at rated conditions.

• If it is a full discharge → Rated charging time

Discharge test time: duration of single transient test removing energy from the device

Discharging time between 2 different storage levels: duration of single transient test removing energy from the device between 2 storage levels.

- If the HTF flows in nominal conditions →Nominal discharging time
- If, in addition, it works between minimum and maximum storage levels → Characteristics nominal discharging time

Discharging time²: duration of single transient test removing energy from the device between 2 storage levels at rated conditions

 If it is a full discharge → Rated discharging time

Heat loss rate: heat loss per degree temperature difference between the average storage medium and ambient temperature

Thermal losses at a temperature: power thermal losses of the device to ambient, while the former is at a certain temperature. Idle thermal losses along a time: power thermal losses to ambient along a time interval

Dynamic Thermal Losses at a temperature: power thermal losses of the device to ambient, while the former is at a certain temperature. (Energy Balance Method) Idle or stationary thermal losses along a time: power thermal losses to ambient along a time interval (2 methods: Isothermal and Cold down)

Table 2KPIs of the different standards and guidelines currently available. ¹It is not considered as a KPI but it is mentioned; ² Highlighting the influence of the initial conditions on the obtained value for this parameter; ³ This is a 1st Law Thermodynamic approach.

ANSI/ASHRAE 94.3–2010 (Sensible)		(TSC): volumetric heat capacity of all invelope, including HTF (no insulation	dimensional temperature, and time	$\frac{dr-0,632}{0,368}$ where ϕ and τ are non- e, respectively, based on Theoretical Storage ixed) $\leq S \leq 1$ (perfectly stratified)
ANSI/ASHRAE 94.1–2010 (Latent)		Storage efficiency: discharge capacity divided by charge capacity		
SFERA		Thermal efficiency at a time t^* : discharge capacity divided by charge capacity when time t^* has passed between charge and discharge	Response time at charge/ discharge: time required for the device to achieve the maximum discharging power at nominal conditions	Comparison factor (CF): ratio between the ideal and measured times in discharge. By 'ideal' is understood the time obtained from certain theoretical model considering homogeneous temperature at the storage medium, ideal heat transfer to the HTF and no thermal losses. CF is a figure that indicates not only how far the device behaves from an ideal situation but also how good the proposed theoretical model is.
SFERA-III	Theoretical Storage Capacity (TSC) ¹ : volumetric heat capacity of all components of the device, including HTF. Related to Utilization Rate	Storage efficiency ^{2,3} : discharge capacity divided by charge capacity while they are consecutive processes. If nominal conditions are considered and the processes take place between minimum conditions, then it is called Rated Storage Efficiency		

inlet and outlet had a difference lower than 1 $^{\circ}$ C (i.e., charging process was defined by the PCM temperature). TES/Charge Efficiency was the ratio between the theoretical (maximum) heat storage capacity and the energy given during a charging process. This TES/Charge Efficiency concept differs from others TES efficiency definitions in considering the Theoretical Storage Capacity instead of the real discharge capacity or storage capacity.

He et al. [29] proposed and tested a two-layered high temperature PBTES prototype having as filler two kinds of PCMs, each of them with different size in their spherical macro encapsulation. They used the prototype in an unusual way, because, in charge, the hot air (375 °C) flowed upwards from the bottom, while in discharge air flowed downwards from the top of the tank. With this way of operation, it was impossible to achieve and maintain a thermal stratification exploiting the air buoyancy forces. Both the charging and discharging times were fixed to 250 min. The average charging and discharging rates were given based on the HTF temperature difference. The Energy Storage Efficiency was defined in the same way as in [27]. The Release Heat Efficiency was defined as the discharged energy, based on HTF temperature difference and the maximum heat storage capacity. They called Overall Efficiency of the Charge-Discharge Process within the same time to the ratio between energy given by the prototype to the energy given to it, which is the Storage or Thermal Efficiency in ANSI/ASHRAE 94.1.2010, SFERA and SFERA-III protocols.

Xie et al. [30] experimentally analysed epoxy resin-based composite PCM in a packed-bed thermal energy storage device for ventilation having air as the HTF and using a dimensionless evaluation method. They defined the *Normalized Energy of Material* as the ratio of the actual stored /released heat to the theoretical value based on material temperatures. The article mentioned the *Utilization Efficiency* as the rate of the stored energy to the energy released using the HTF temperatures.

Lu et al. [31] proposed a novel two-stage latent TES for heating systems. Numerical simulations provided the optimized cascade mode and the most adequate PCMs. A prototype was tested, using experimental results for validating the model simulations and for comparison with other latent storage devices for heating systems. They used as figures of merit *Heat Transfer Efficiency in Charge* or *Discharge*, as the ratio of the thermal energy stored by the PCM to the thermal energy released by the HTF (water) or as the ratio of the thermal energy gained by the HTF and the thermal energy released by the PCM, respectively. They also

used the *Heat Storage Release Ratio* as the ratio in discharge power to charge power based on HTF in a full discharge and charge cycle, i.e., the same as the *Storage/Thermal Efficiency* defined in ANSI/ASHRAE 94.1.2010, SFERA and SFERA-III protocols. When comparing the obtained values, they talked on higher/lower thermal utilization efficiency.

Shen et al. [32] studied the thermodynamic performance of a low-temperature cascade latent TES with 3 PCMs in series in a finned-tubes and shell configuration using the *Energy Efficiency during Charging Process*, as the ratio of the energy gained by the PCMs in charge to the energy gained by the HTF (air) in discharge. According to the figures shown in the study, the charging time seemed to be the time for which the difference in temperature at the inlet and outlet of the HTF in the three stages of the PCM was nearly zero. They also used the *Exergy Efficiency during Charging Process*, as the ratio of the exergy gained by the PCMs in charge to the exergy gained by the HTF in discharge.

Fan et al. [33] analysed the performance of cascade latent TES prototypes with three different paraffin based PCMs stages and layouts of HTF tubes. To compare the behaviour of the different prototypes they used the *Heat Charge Efficiency*, as the ratio of the energy gained by the PCMs to the heat provided by the HTF. Additionally, they used the *Exergy Charge Efficiency*, as the ratio of the exergy gained by the PCMs to the heat provided by the HTF, assuming it is an ideal liquid with stable flow.

Salem et al. [34] tested a latent TES prototype using an organic paraffin, RT60, as PCM, with a vertical shell-tube heat exchanger configuration. To define the limits of charging and discharging processes they used both the temperature of the PCM and the HTF outlet temperature. Thus, charge (discharge) was assumed to finish when the lowest (uppermost) location temperature at PCM reached its melting point and/or when the HTF outlet temperature did not change for 20 min. Charges/Discharges were assumed to start when the average PCM temperature reached PCM melting point (in this case 58 °C). In other words, the PCM temperature imposed the start and end of the processes. Charging Efficiency was the ratio between the real heat energy stored within the PCM and the theoretical one, i.e., assuming that the PCM would have the same temperature as the HTF at its inlet during charge. This way of defining the charging efficiency is the inverse of what Li et al. [27] proposed. In a similar way, Discharging Efficiency was estimated as the ratio between the real and maximum energy released by

the PCM.

Lu et al. [35] established the end of charge of a shell-tube latent TES prototype with fins when the HTF (water) outlet temperature variation remained within 1 °C for 10 min or time reached 8 h. Discharging time was fixed to 7 h. As KPIs they proposed the *Total Heat Storage Capacity* as the energy provided by the HTF in a charging process (*Charge Capacity* in ANSI/ASHRAE 94.1.2010, 94.3.2010, SFERA and SFERA-III protocols), the *Average Heat Storage Power* as the ratio of the total heat storage capacity to the charging time, *Effective Energy Release Efficiency* as the ratio of the discharging capacity (heat absorbed by the HTF in a discharging process) to the total heat storage capacity (what it is meant as *Storage/Thermal Efficiency* in ANSI/ASHRAE 94.1.2010, SFERA and SFERA-III protocols).

Lázaro et al. [36] identified the difficulty in comparing different heat transfer enhancing mechanisms in latent (solid-to-liquid) TES devices, proposing a method for comparing different TES prototype conditions, configurations and sizes. This method used the Energy Storage Capacity of the System -as defined by IEA-ECES Annex 30 [21]-, the Energy Storage Density as the ratio of the energy storage capacity to the total volume of the device, including insulation and vessel, and a Normalized Power using the total volume of the device and a reference temperature difference. This approach was used as methodology in Subtask 4P of the IEA SHC task 58/Annex 33 [37]. König-Haagen et al. [38] analysed eleven latent storage systems with different designs and sizes and under different boundary and initial conditions with this methodology, using as reference temperature the melting and the initial temperature. The work confirmed how critical the choice of the reference temperature was, claiming that neither of the two options led to completely fair results for the sensible and latent heat parts. To overcome this drawback, the possibility of weighting the reference temperature in the calculation of the mean value according to the latent and sensible parts was mentioned and it was proposed to be studied in the future.

2.2.2. Characterization of sensible heat prototypes

Sensible heat prototypes are those that store heat by increasing the temperature of a fluid or a solid material without changing its state. The followings are the most recent works dealing with this concept.

Soprani et al. [39] evaluated the performance of PBTES with rocks as filler and considered the Thermal Storage Capacity based on the achieved maximum temperature of the storage material (450 kWh_{th}). The HTF was air heated by electric heaters up to 600 °C. They used as main KPIs what they called First Law Charging Efficiency and Round Trip (Discharging) Efficiency, which are both calculated through the energy given to, or provided by, the filler based on its temperature evolution, and the required electrical energy for both heating and moving the air. When it is the energy given to, or provided by, the air HTF, they referred to the Second Law Charging and Round Trip (Discharging) Efficiencies. In both cases, the definitions are far from the respective (or similar) KPIs considered in ANSI/ASHRAE 94.1.2010, SFERA and SFERA-III protocols. As the authors pointed out, considering the energy stored only in the rock filler, when it is a prototype where the energy stored 'outside' the rock-bed may be significant, gives inconsistent results of charge efficiency, which may become lower than round trip efficiencies, which has no sense. Heat losses were obtained experimentally and using modelling.

Ortega-Fernández et al. [40] erected and tested a 400 kWh_{th} packed-bed prototype with slag particles of an average size of 1 cm. They focused their attention on the air pressure drop along the packed-bed and on the thermal losses as parameters to study the performance of the prototype.

Zhou et al. [41] tested three types of filler (ore particles, alumina and rock gravel) in a packed-bed tank of 0,85 m high (bed height of 0,65 m) and inner diameter of 0,32 m. To compare the energy performance of what may be considered three prototypes (the same tank with different fillers) they looked at the evolution of temperatures, *Charging* and *Discharging Times*, and *Charging*, *Discharging and Cycle Efficiencies*. They

considered that charge stopped when the outlet air temperature reached 0,65 times of the predetermined inlet air temperature. While discharge stopped when the air outflow temperature dropped below 60 °C. The Charging and Discharging Efficiencies are those that Soprani et al. [39] named as Second Law Charging and Round Trip Efficiencies, respectively. Cycle efficiency, also named energy recovery efficiency, was defined as the ratio of the heat released to the air HTF during discharge to the total energy consumption in a complete charge-discharge cycle. The total energy consumption contained the input thermal energy and the pumping work during both charge and discharge. Additionally, they calculated a Stratification Number as the ratio of the average temperature gradient at any time to the maximum average temperature gradient during charge. This definition is pretty different than the similar KPI that only is mentioned in ANSI/ASHRAE 94.3–2010 and named as Stratification Index.

Trevisan et al. proposed an innovative approach for PBTES based on a radial flow concept. They tested a 49.7 kWhth prototype at working temperatures between 25 °C and 700 °C and Denstone 2000® particles with a hydraulic diameter of 6 mm as filler [42,43]. The considered KPIs to compare the prototype performance under different operating conditions are the Stored Energy, calculated by dividing the bed in 25 volumes and assuming the mean temperature of them as the achieved temperature in relation to the (homogeneous) initial one; the State of Charge, SOC, at a given time, as the ratio of the actual energy stored in the filler to the maximum theoretical energy; the Charge Efficiency, as the ratio of the stored energy of the whole bed and the energy provided by the HTF in relation to a reference temperature given by the inlet temperature at discharge; the Discharge Efficiency, as the ratio between the energy provided to the HTF along the prototype and the stored energy during charging; the Total Efficiency, as the product of the above two efficiencies; the Utilization Rate, as ratio between the utilized storage capacity and the maximum one for each operation cycle. The Temperature Uniformity Index was introduced as a specific KPI for radial flow packed-beds, to study the uniformity of the temperature along the axial, vertical direction.

Knobloch et al. [44] considered, like [39], the *First Law* and *Second Law Charge* as well as *Round Trip (Discharging) Efficiencies* as figures of merit to characterize a high temperature energy storage based on rocks, partially underground and with air as HTF, heated by electric resistance up to 675 °C. They defined a discharge cut-off temperature, which was assumed to be the ambient temperature of 0 °C (the pilot plant is located in Sweden). They added as another figure of merit the *State of Charge, SOC*, at a given time, in the same way as Trevisan et al. [43]. The end of a charge or discharge was defined by having around 60–80 % *SOC*.

Okello et al. [45] studied the performance of a TES prototype that contained a combination of PCM (eutectic mixture of NaNO3 and KNO3) and rock particles in a single packed-bed, with air as HTF (details on design and constructions are available at [46]). They compared its behaviour with the experimental behaviour of a rock bed by means of what they defined as the Capacity Ratio, or ratio of the energy stored in the TES device, based on averaging thermocouples readings along the axial bed length, to the theoretical maximum energy the device can store (i.e., assuming the device is at a uniform temperature equal to the inlet HTF temperature in charge). The problem of supporting the KPI of a TES device on the temperatures of the storage material is to what extent these temperatures are sufficiently representative of the whole storage material, given the limitation of instrumentation in both number of temperature gauges and their locations. The Rate of Heat Loss of the bed as a function of time in an idle process was also based on the previously defined stored energy.

Rao et al. [47] experimentally studied three lab-scale sensible prototypes with concrete as storage medium and different HTF pipes materials and geometries. They compared the following performance parameters between the three prototypes: Charging/Discharging Time, as the time the storage medium requires reaching the same HTF inlet temperature; the Effective Charging/Discharging Time, time required to

achieve a volume average temperature of the solid media 5 degrees higher/lower than the HTF inlet temperature; and the *Energy Stored/Discharged*, both based on the initial and average volumetric storage media temperature. The average volume temperature was obtained by 9 thermocouples arranged in 3 sections, one located close to the inlet, another in the middle and the third one close to the outlet. The thermocouples were at half of the distance between the prototype axis and its outer surface. Considering that the prototypes were 1 m long and around 30 cm diameter, in the authors' opinion, it is quite unlikely that the locations of these only 9 thermocouples were good enough to be representative of what is happening in the core of each prototype.

2.3. Metrics summary and objective

As summarized above, there are a large number of figures of merit or KPIs, different standards and guidelines in the literature without a consensus of the scientific community for the evaluation and comparison of TES prototypes, especially for electricity generation and for industrial process heat above 180 °C. The lack of definition in the most adequate KPIs avoids a proper comparison between different studies and/or prototypes. The SFERA-III project represents a significant intent in addressing this gap by proposing a standardized methodology for assessing TES systems. While the project has validated these KPIs across several TES devices, none have been applied to a packed-bed system until now.

For this reason, the main objective and innovation of this research is to assess the feasibility of the procedure proposed in the SFERA-III project, as one the most recent and updated test guidelines, to evaluate the KPIs of thermal storage prototypes in a specific packed-bed device, which is one of the most studied TES due to their potential for industry, to establish a baseline for the comparison of packed-bed prototypes. To demonstrate the extent of the applicability of the testing guidelines, the experimental cases incorporate various operational parameters, such as air mass flow rates and maximum charging temperatures.

The challenges encountered during the process are elucidated, as are the various solutions proposed and their impact on the resulting KPIs. Furthermore, the differences observed following the aforementioned procedures are emphasised, mainly with regard to the definition of charging/discharging time. To date, only a published study has explicitly applied the SFERA-III KPIs to a 300kWh_{th} latent storage prototype [48]. It is the authors' hope that this work will contribute to reinforce a common language within the scientific community for testing TES prototypes by completing the validation of the SFERA-III procedures with another TES prototype type, a packed-bed device. This will contribute to the advancement of knowledge not only of packed-bed systems but also of thermocline storage tanks, and in the establishment of updated KPIs.

3. TES prototype description: Sensible packed-bed

The ALTAYR facility is a sensible packed bed originally designed to test energy storage materials [49,50], or to validate simulation models [51], using air as HTF for application in concentrated solar thermal (CST) technologies. The CST plants using air as HTF can increase their operating temperatures above the current state-of-the-art, which are molten salts operating at 565 $^{\circ}$ C, in order to improve the overall plant efficiency. Therefore, the ALTAYR facility was planned to operate at nominal working conditions with higher temperatures than current state-of-the-art technologies. The nominal conditions initially set are as follows:

- \bullet An air temperature at the inlet of the charging process of 700 $^{\circ}\text{C}.$
- A mass flow rate of 75 kg/h
- A heating capacity of 15 kW.

However, the ALTAYR packed bed can operate in working conditions different from the nominal ones, being the limits as follows:

- \bullet The maximum temperature limit is set at 900 $^{\circ}$ C, which is the upper limit supported by the electrical resistances.
- The maximum air mass flow rate limit is set at 100 kg/h, which is the upper limit supported by the blower.

In this research, the experimental data obtained from the ALTAYR facility after testing a ceramic filler serve as basis to evaluate the KPIs proposed in D6.3 of SFERA-III project.

ALTAYR's main component is a stainless-steel vessel (Fig. 2–1) with a bed volume of around 0,1 m³ (bed height and inner diameter of both 0,5 m). It consists of a metal casing with a thick ceramic inner insulating wall. Above and below the cylindrical main body there are two additional conical bodies coinciding with the air inlet and outlet. In a charging process, the ambient air is heated by a set of electric resistances of 15 kW -there is not a recirculation loop-. Although the electric heaters box (Fig. 2–4) is close to the ground, during the charge the hot air is introduced into the tank from the top through a pipe (Fig. 2–3 in blue), going through the packed-bed, and exiting the tank from the bottom, to be finally poured to the environment by a flexible pipe (Fig. 2–3 in black). During the discharge, the air path changes the direction, entering the packed-bed at the bottom and exiting at the top.

While temperatures and mass flow are recorded every 30 s with a data logger, electric power consumption is manually recorded.

The tank is provided with thermocouples within the filler material and in the vessel (Fig. 2–2). There are 45 thermocouples inside the tank, which are located at 9 levels with 5 measurement points at each level: one at the vessel axis and the other four at different distances from the vessel axis (Fig. 3). The temperature of the external surface of the insulated vessel is measured at 10 levels and 5 different angular positions per level. The air HTF temperature is measured at its inlet and outlet.

In this study, RethinK Seramic Flora® was used as filler material and around 130 kg were introduced in the storage tank. RethinK Seramic Flora are flower-shaped ceramic pieces made from heavy industry waste (Fig. 4). Table 3 presents the main properties of the filler material according to the provider. The porosity given by the provider has been increased up to 0,5 to consider the volume occupied by the thermowells.

4. General description of the tests

According to SFERA-III guideline [23], the main temperature measurements are made on the HTF side, thus outside of the storage vessel. This approach allows for easy measurements, and it is consistent with the system control. Additionally, characterising a TES device based on temperature measurements on the energy storage material entails inherent inaccuracies due to the limitation imposed by representing the whole mass of energy storage material by a certain number of temperature gauges at certain locations, as previously highlighted in the studies of Rao et al. [47] and Okello et al. [45]. Energy storage material temperatures can be used to check the reliability of the HTF temperature measurements -as in this study-, to check or improve simulation models, to enhance the device design, etc., but, according to the authors' knowledge, it is not useful when the objective is the actual characterization of a TES device by means of certain figures of merit.

As pointed out in SFERA-III guideline, the KPI values depend on the initial state of the TES device, especially if it is a packed-bed (HTF is a gas so its thermal energy storing capability is negligible) or a thermocline (HTF is a liquid so it also stores enough thermal energy to be considered). The guideline considers the possibility that the device was in what is called, steady-state conditions, i.e., when there is no variation of the parameters/measurements over time. These conditions do not mean that the TES system is at a uniform temperature, but that a thermal gradient may exist, as long as it does not change significantly over time.



- Storage tank where the filler is allocated
- 2. Thermocouples
- 3. Air pipes
- 4. Electric heaters box
- 5. Blower
- 6. Flowmeter
- 7. Control Valve
- 8. Control Board
- 9. Power Consumption board

Fig. 2. Picture of ALTAYR packed-bed experimental facility with all its components, adapted from [52].



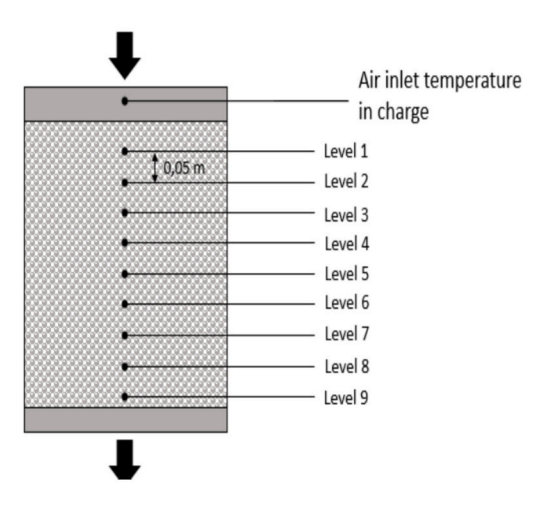


Fig. 3. View and scheme of the interior of the ALTAYR tank with the thermocouples at different locations (no filler in yet).





Fig. 4. View of the interior of the ALTAYR tank partially (left) and totally (right) filled with the ceramic pieces used as filler.

"Significantly" means that stable conditions are ensured, implying that a given variable does not change more than a certain value over a certain period of time (if temperature is the measured magnitude, 1 to 5 K is suggested as an affordable variation along 1 to 5 % of the real or theoretical charging/discharging time). The possibility of having a (stable) thermal gradient as a starting point for the testing of a storage device is only being considered in the SFERA-III guideline.

The aim of this experimental campaign is to check the KPIs of the SFERA-III project for different operational conditions set in the charging process: different air mass flow rates and different air inlet temperatures. In this regard, the packed-bed was tested under two different set of tests:

firstly, at a constant air mass flow rate, $50 \, \text{kg/h}$, that allows us to operate at air inlet temperatures at the charging process, ranging from 700 to $850\,^{\circ}\text{C}$ (close to the upper limit supported by the electrical resistances as presented in section 3), and secondly, at the nominal temperature of the air at the inlet of the charging process of $700\,^{\circ}\text{C}$, under different air mass flow rates ($50-60-70 \, \text{kg/h}$). This mode of operation means that both the charging and discharging processes start with a stable thermal gradient (steady-state condition). Each charging test was followed by a discharging test at the same air mass flow rate as the charging test. With these two sets of working conditions, the ceramic filler material is sufficiently tested, and the results are useful to checking and discussing the

Table 3Properties and characteristics of the filler material (RethinK Seramic Flora®, provided by Seramic Materials Ltd. [53], and in accordance with [54,55]).

Property	Provider info
Composition	Al ₂ O ₃ (min. 35 %), ZrO ₂ (max. 25 %), SiO ₂ (max. 40 %), Fe ₂ O ₃ + TiO ₂ (max. 5 %), K ₂ O + Na ₂ O (max. 5 %), CaO + MgO (max. 1 %)
Bulk density (kg/m ³)	2700
Porosity	0,45-0,47
Packing density (kg/ m ³)	1458
Specific heat (J/kg·K)	1024
Characteristic length (mm)	40

SFERA-III KPIs.

Table 4 compiles the operating parameters of the tests performed, ordered sequentially according to the way in which they were carried out. Although the sequence of tests shows first the charging tests followed by the discharging tests, this study presents and discusses first the discharging tests (section 4.1), as the authors are aware that they are the most important and critical to study when testing (or designing) a thermal storage device or prototype. Of course, the charging processes (section 4.2) are important, as they define the stored energy in the device, but how this stored thermal energy is delivered to the application (discharging process) is the main point that decides the feasibility of a thermal storage device. Within each section, there are tables with specific data related to discharging or charging tests, which enrich the analysis with valuable information essential for a comprehensive interpretation of the results.

4.1. Discharging tests

Several full discharging tests have been carried out with different mass flow rates and air inlet temperatures. Fig. 5 shows the temperature profiles for test #2 discharging process, as an example. Temperature profiles for discharging tests #4, #6, #8, #10 and #12 are shown in Appendix A.

In all discharging tests performed, process starts from what is called 'steady-state end of charge', whereby not all the storage volume is at uniform temperature, but there is a thermal gradient along the packed-bed. The initial conditions are, therefore, 'steady-state full charge state'. As can be seen in the example given in Fig. 5, the air outlet temperature (T_{out}) has a thermal inertia that delays the decrease of this temperature value.

The first thing to look at is the **discharging time**, as it defines many other KPIs. In the SFERA-III guideline, the definition of the end of a complete discharging process is open to different criteria, as long as it is clearly stated and followed. Considered as a non-exhaustive list, the following criteria are suggested for sensible storage devices:

 Table 4

 List of experimental tests and their operational parameters.

Test	Туре	Air mass flow (kg/h)	Rated temperatures (°C) (T_{in} , in charge and T_{out} in discharge)
#1	Charge	50	710
#2	Discharge	50	700
#3	Charge	50	760
#4	Discharge	50	750
#5	Charge	50	810
#6	Discharge	50	800
#7	Charge	50	855
#8	Discharge	50	850
#9	Charge	60	715
#10	Discharge	60	700
#11	Charge	70	715
#12	Discharge	70	700

- 1. When the specific enthalpy of the outlet HTF is equal or below a defined threshold. This threshold is usually given by the application in which the storage prototype will be integrated.
- When the specific enthalpy difference of the HTF between inlet and outlet becomes constant for a mass flow rate (a steady-state end of discharge).

Since the prototype used in this work stores sensible thermal energy, the estimation of the specific enthalpy of the HTF is based on its temperature. Fig. 5, as an example of a discharge, shows that the air temperature difference between the inlet and the outlet follows an asymptotic tendency to zero. Defining the end of discharge with the second criterion (the difference between inlet and outlet becomes constant for constant mass flow rate) imposes a very long discharging time, which may not represent properly the usefulness of the device. Therefore, the first criterion has been assumed and a discharge ends when a specific threshold of the temperature difference between the inlet and outlet is reached.

Table 5 shows, for the discharging tests listed in Table 4, the results using different thresholds in such a temperature difference. If a threshold of 5 °C is defined, the discharging time is presented as t_{dI} . If a temperature difference of 3 °C was considered, the discharging time increases by about 2 h. If for defining the end of the discharge, the temperature difference inside the packed-bed (T_{levelI} - T_{level9}) was 5 °C or lower, the discharging time (t_{d2} in Table 5) would be reduced by 3 to 4 h. However, if the threshold is defined based on having a discharge enthalpy of 70 % of the gained enthalpy by the storage device, as Weiss did when testing its solar salt thermocline without filler [26], i.e., at T_{out} , $t_{d} = T_{out, rated} - 0.7$ ($T_{out, rated}$ - $T_{in, rated}$), the discharging time (t_{d3} in Table 5) is much smaller than considering the threshold 5 °C in outlet-inlet air temperature difference.

Therefore, it seems critical to establish clearly what the minimum temperature/enthalpy difference is affordable for the specific application for which the TES device is designed. While power generation is a very exigent application, as the efficiency of the power block is greatly affected by any input temperature variation, industrial process heat is a much more relaxed application, whenever the temperature is kept within certain operational limits. Furthermore, having a clear idea of the boundaries that defines the end of discharge can be critical when designing the TES device, not only because these boundaries will define the required oversizing, but also because it can force the design and operation of the system surrounding the TES device. In the device considered in this work, having a limit of 5 °C or 3 °C for the temperature difference between the inlet and outlet air implies that in a discharge the thermocline region is practically extracted out of the tank. However, if the end of the discharge is based on a discharge enthalpy of 70 % of the gained enthalpy, part of the thermocline region remains inside the tank. If a charging process started from that situation, it is well known, not only for packed-beds [56], but also for thermocline tanks [57], that the stratification within the tank would decrease, as well as its capacity to store energy. Therefore, the complete extraction of the thermocline region is desirable, and the heat contained in this region should be directed to somewhere useful (e.g., preheating of certain equipment nearby) with the related changes in the overall system scheme.

4.2. Charging tests

Several full charging tests have been performed with different air mass flow rates and inlet temperatures. Fig. 6 presents the temperature profiles along the test #1 charging process as an example. Temperature profiles for charging tests #3, #5, #7, #9 and #11 are shown in Appendix B.

Table 6 shows the tests selected to evaluate the performance of the prototype with some related information: the air temperature difference between its inlet and outlet (T_{in} - T_{out}), the maximum measured air inlet temperature, $T_{in,max}$, the maximum measured temperature within the

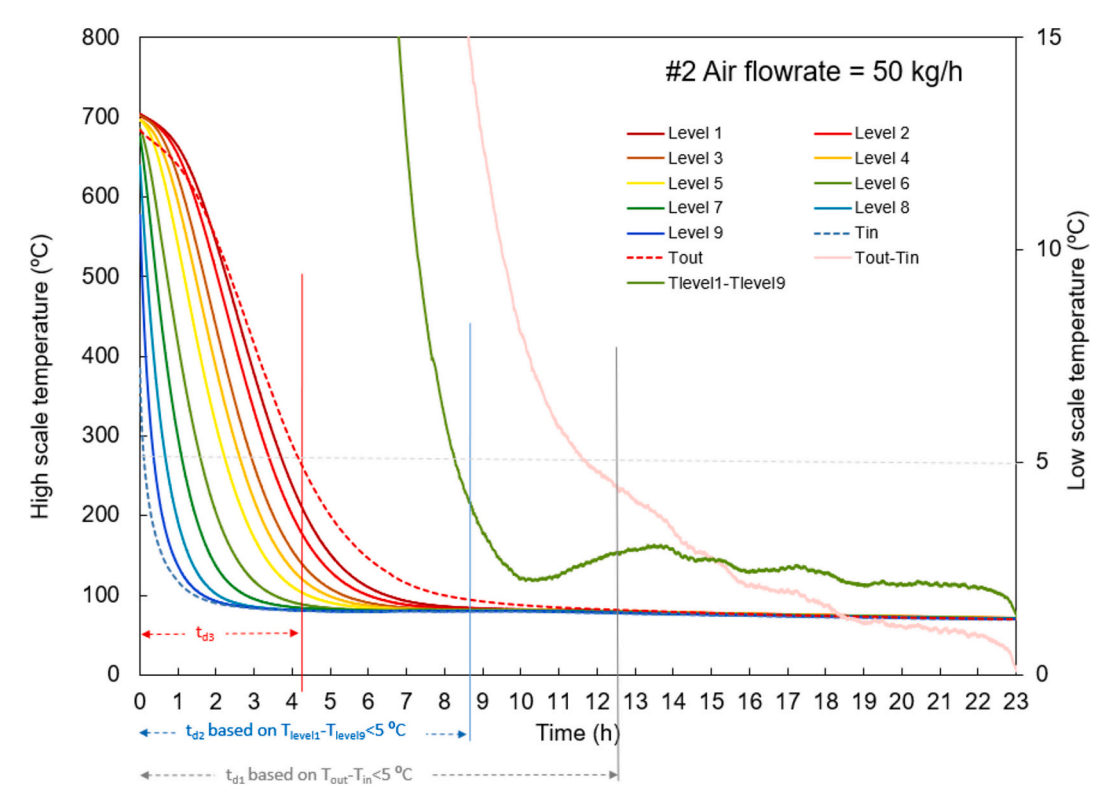


Fig. 5. Discharge #2. Low temperature scale for temperature differences (T_{in} - T_{out}) and (T_{level1} - T_{level9}). Level 1 refers to the uppermost part while level 9 refers to the lowest part of the packed-bed (see Fig. 3).

Table 5Discharging processes and some related information.

Test	Air mass flow (kg/h)	$T_{in,max}$ (°C)	T _{out,max} (°C)	$(T_{out}$ - $T_{in})_{\max}$ (°C)	<i>t</i> _{d1} (h)	<i>t_{d2}</i> (h)	<i>t_{d3}</i> (h)	$T_{level1,max}$ (°C)	$T_{level9,min}$ (°C)	$(T_{level1} ext{-}T_{level9})_{ ext{max}}$ (°C)
#2	50	384,4	683,9	522,1	11,7	8,3	4,1	704,4	577,3	527,3
#4	50	660,5	752,2	553,1	12,6	8,8	4,1	758,8	707,8	557,9
#6	50	621,5	784,3	588,8	12,3	8,8	4,1	806,6	737,3	592,9
#8	50	736,9	843,4	627,3	13,0	9,0	4,2	850,0	787,9	630,2
#10	60	576,9	688,9	536,1	10,5	6,8	3,4	707,5	662,9	544,2
#12	70	591,7	690,2	544,5	9,6	5,9	3,1	707,3	671,6	545,6

packed-bed, $T_{pb,max}$, the packed-bed mean temperature when a stationary condition is achieved, $T_{pb,ss}$ and the estimated charging time, t_{ch} .

For each charging process (see Appendix B or Fig. 6 as an example), when a stable condition is achieved, the air inlet temperature measured value is a little bit below the measured temperature of level 1, indicating that the location of this thermocouple is a cold spot that does not accurately represent the air inlet temperature. The shape of this air inlet temperature at the inflexion point before reaching a constant value is because the control system of the electric heaters generates slight fluctuations both in power and air temperature before achieving the specific air temperature set point.

Like the discharging processes, the temperature difference between the air inlet and the outlet, T_{in} - T_{out} , follows an asymptotic behaviour. In test #1 this difference is around 83 °C (see Appendix B for the rest of the tests). Defining the end of charging processes when "the HTF specific enthalpy difference between inlet and outlet becomes constant for constant mass flow" imposes a very long charging time, misleading the actual thermal performance that the device may have. Therefore, following what was done for discharging processes, it has been assumed that the charging processes end when the asymptotic temperature value plus 5 °C temperature difference or lower is reached, defining the charging time, t_{ch} , of Table 6. If 3 °C is added to the asymptotic value of temperature difference, each charging time is increased by about 1 h.

5. Finding SFERA-III key performance indicators

Following the discussion on the charging and discharging times, the measurable performance indicators proposed in the SFERA-III guideline are calculated. They are the Storage Capacity, Mean Thermal Power, Utilization Rate, Thermal Losses, Storage Efficiency, Storage Exergy Efficiency, and Auxiliary Power Consumption. To obtain the Utilization Rate, it is necessary to previously calculate the Theoretical Storage Capacity, which has no mayor sense but in its relation to the Storage Capacity. Therefore, it is not considered a KPI itself but a needed 'intermediate' parameter, as in SFERA-III guideline is proposed.

Storage capacity, *SC*, is defined as the amount of thermal energy that the thermal storage system can supply to the HTF in a full discharging process under well-defined conditions. For each test, it is calculated as follows:

$$SC = \sum_{i=2}^{n_d} (t_i - t_{i-1}) \frac{(P_i + P_{i-1})}{2},$$

where ' n_d ' is defined by the end of each discharging process (t_d) and P_i is the thermal power provided by the HTF at time t_i ,

$$P_i = \dot{m_i} \int_{T_{in,i}}^{T_{out,i}} c_{p,HTF}(T) dT$$

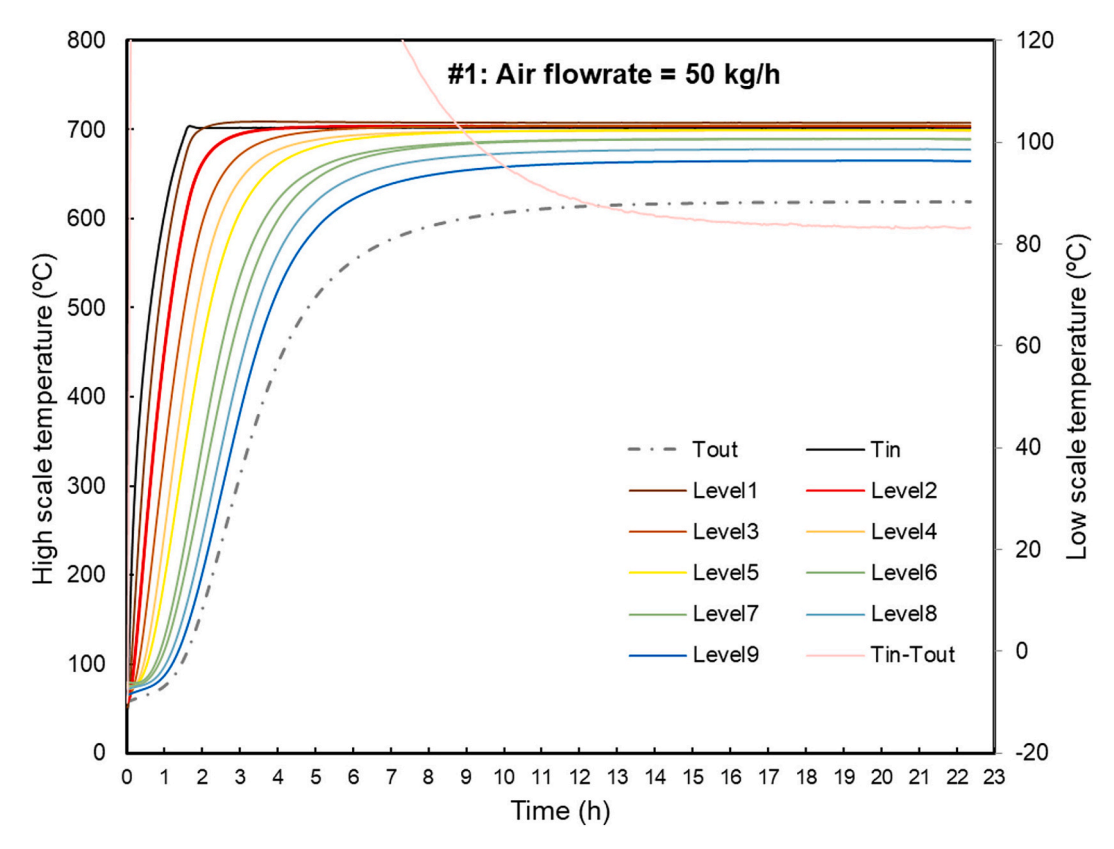


Fig. 6. Charging process #1. Level 1 refers to the uppermost part while level 9 refers to the lowest part of the packed-bed.

Table 6Charging processes and some related information.

Test	Air flow (kg/h)	$(T_{in} - T_{out})_{ss}$ (°C)	T _{in,max} (°C)	$T_{pb,max}$ (°C)	$T_{pb,ss}$ (°C)	<i>t_{ch}</i> (h)
#1	50	83	704,1	708,7	690,8	12,24
#3	50	92	754,2	761,0	741,2	12,35
#5	50	100	804,4	808,5	788,6	12,81
#7	50	107	846,0	852,0	696,5	14,48
#9	60	71	703,4	711,4	696,6	11,60
#11	70	61	703,3	711,4	696,5	10,19

As mentioned before, it is the discharge the primary process that defines the feasibility of a thermal energy storage device for a specific application. Therefore, its Storage Capacity is based on the discharged energy by the HTF, rather than on the energy provided by it in charge or even stored as many authors have proposed ([21,35], for example, of the references mentioned in the Introduction).

Since the HTF is air, it is assumed that $c_{p,HTF}\left(\frac{J}{kg\cdot K}\right)=0, 2\cdot T(^{\circ}C)+990$, obtained by a linear fitting of the published experimental air thermal capacity in the temperature range 700–800 °C. Therefore,

$$\begin{split} P_i &= \dot{m_i} \int_{T_{in,i}}^{T_{out,i}} (0, 2T + 990) dT \\ &= \dot{m_i} \left[0, 2\frac{1}{2} \left(T_{out,i}^2 - T_{in,i}^2 \right) + 990 \left(T_{out,i} - T_{in,i} \right) \right] \end{split}$$

Table 7 shows the storage capacities of the discharging processes here considered, depending of the discharging time considered and according to Table 5.

Associated to discharging time and the Storage Capacity is the **Mean Thermal Power**, P_{mean} , or mean thermal power of a discharging process:

$$P_{mean} = \frac{SC}{t_d}$$

Table 7 shows also the mean power values considering different discharging times.

If the end of discharging processes was considered when the air temperature difference at its inlet and outlet is 3 °C or when P_{i+1} - P_i < 0 (implying discharging times between 18 and 23 h), SC values not higher than 1–2 % of those reported in Table 7 are found. Comparing the Storage Capacities obtained according to the different definitions of discharging time for each working condition, a maximum deviation of

Table 7
Storage capacities calculated assuming different discharging times: t_{dI} (obtained when $(T_{in} - T_{out}) \le 5$ °C), t_{d2} (from $(T_{levelI} - T_{level9}) \le 5$ °C), t_{d3} (from $T_{out,d} = T_{out,rated} - 0.7$ ($T_{out,rated} - T_{in,rated}$).

Test	Air mass flow (kg/h)	<i>t</i> _{d1} (h)	$SC(t_{d1})$ (kWh)	P_{mean} (t_{d1}) (kW)	t _{d2} (h)	<i>SC</i> (<i>t</i> _{d2}) (kWh)	P_{mean} (t_{d2}) (kW)	<i>t</i> _{d3} (h)	$SC(t_{d3})$ (kWh)	P_{mean} (t_{d3}) (kW)
#2	50	11,7	29,22	2,50	8,3	28,78	3,47	4,1	24,3	5,93
#4	50	12,6	30,94	2,45	8,8	30,41	3,46	4,1	25,6	6,21
#6	50	12,3	32,80	2,66	8,8	32,36	3,68	4,1	27,3	6,69
#8	50	13,0	35,89	2,76	9,0	35,36	3,93	4,2	29,7	7,11
#10	60	10,5	25,14	2,39	6,8	24,58	3,61	3,4	20,9	6,08
#12	70	9,6	23,15	2,42	5,9	22,52	3,82	3,1	19,2	6,15

17 % is obtained. When comparing different conditions but the same discharging time definition, the deviation increases up to 22 %. This relatively small dispersion of storage capacity values with working conditions implies that the longer the discharging time is –depending on the threshold defined-, the smaller the mean thermal power values.

Theoretical storage capacity, *TSC*, is defined as the maximum amount of energy that the materials in the storage system can accumulate from a thermodynamic point of view. It is an ideal parameter in which no heat losses nor stratification is considered [23]. The materials to be considered are not only the storage media, but also the walls, insulation, etc. of the device itself. In the study here presented, the tank walls, including refractory bricks (referred with the subscript RB), insulating fibre (subscript IF) and outer steel envelope (subscript SE) are considered for all the components that make up the ALTAYR facility (Fig. 2 and Fig. 3). Therefore, the following expression defined the theoretical storage capacity:

$$\begin{split} \textit{TSC} &= \left[\left(\textit{mc}_{\textit{p}} \right)_{\textit{filler}} + \left(\textit{mc}_{\textit{p}} \right)_{\textit{RB}} + \left(\textit{mc}_{\textit{p}} \right)_{\textit{IF}} + \left(\textit{mc}_{\textit{p}} \right)_{\textit{SE}} \right] \left(T_{\textit{rated,ch}} - T_{\textit{rated,d}} \right) \\ &= \left[\left(\textit{mc}_{\textit{p}} \right)_{\textit{filler}} + \left(\textit{mc}_{\textit{p}} \right)_{\textit{ALTAYR}} \right] \left(T_{\textit{rated,ch}} - T_{\textit{rated,d}} \right) \end{split}$$

where $T_{rated,ch}$ and $T_{rated,d}$ are the mean temperatures of the inlet and outlet rated temperatures at charging and discharging processes, respectively. The *TSC* depends on these rated temperatures [24]. The rated conditions are established when the thermal storage system is designed, so in the case of the ALTAYR, being a facility for testing packed-bed issues, the rated values with the ceramic filler material are presented in Table 8.

The rated charging conditions have been defined as those reached when the storage system is in stable conditions, i.e., when the temperatures of the HTF at the inlet and outlet do not vary much. Fig. 7 shows, as an example, test #11, that obtaining $T_{in,rated} = 715$ °C and $T_{out,rated} = 640$ °C, so the $T_{rated,ch} = 677.5$ °C.

As mentioned before, the measured air inlet temperature is always a little bit below that of level 1, not accurately representing the air-inlet temperature. That is why the maximum temperature at level 1 is the one used to define $T_{in.rated}$.

For the discharging processes presented in this study, the definition of the rated conditions seems to be a bit more difficult, as the air temperature at the outlet decreases quite fast and the air has to go through the (hot) electric heaters (Fig. 8).

According to Alonso et al. [52], the $(mc_p)_{ALTAYR}$ is 3,75·10⁵ J/K. With this figure, the mass, m, and c_p of the filler and the rated temperatures of Table 8, the theoretical storage capacity, TSC, is calculated for the different tests and shown in Table 9.

What components and elements are considered in the Theoretical Storage Capacity defines critically its value. In devices such as ALTAYR, with so many elements, considering only the tank itself, gives a value of $(mc_p)_{ALTAYR}$ an order of magnitude lower (7,62·10⁴ J/K). If the entrance and exit cones are considered together with the tank, the $(mc_p)_{ALTAYR} = 1,2\cdot10^5$ J/K [50]. Therefore, it is confirmed that it should be stated clearly what elements are considered and what are not, supporting the suggestion given in [23].

 Table 8

 Rated temperatures for charging and discharging processes.

	Charg	e			Discha	Discharge				
Air mass flow (kg/h)		T _{in,} rated (°C)	T _{out,} rated (°C)	T _{rated} , ch (°C)		T _{in,} rated (°C)	T _{out,} rated (°C)	T _{rated} , d (°C)		
50	#1	710	610	660,0	#2	100	700	400		
50	#3	760	660	710,0	#4	100	750	425		
50	#5	810	700	755,0	#6	100	800	450		
50	#7	855	735	795,0	#8	100	850	475		
60	#9	715	630	672,5	#10	100	700	400		
70	#11	715	640	677,5	#12	100	700	400		

The **Utilization Rate**, *UR*, is defined as the ratio, in percentage, of the storage capacity to the theoretical storage capacity,

$$UR = \frac{SC}{TSC}$$

This figure represents the device's capacity to transform the total theoretical energy it is capable of storing into useful energy during a discharge.

Considering the results given in Table 9, utilization rates for this thermal storage device are shown in Fig. 9.

Since the *UR* depends on the *TSC*, and this depends on which elements, materials and components are considered for its calculation, the comparison between different thermal storage prototypes based on their corresponding *UR* does not seem to make sense. On the other hand, *UR* is a quite useful parameter to find out, for a specific prototype, which working conditions obtain the highest thermal potential of the device. Considering the working conditions of the discharging tests, whose *URs* are shown in Fig. 9, it is clear that for specific rated conditions, the higher the mass flow rate, the lower the *UR*, and for a specific mass flow rate, the higher the temperature, the higher the *UR*.

The SFERA-III guidelines proposed 4 different methods to evaluate the **Thermal Losses** in TES prototypes, even though that they can hardly be extrapolated from small to large devices. Some of the methods cannot always be applied:

- a. Isothermal method: The device is maintained at a constant temperature for a specified period of time. The (electrical) energy required to maintain this condition is equivalent to the thermal losses at that temperature. This method requires a heat tracing around the prototype or immersed electric heaters, none of which are available in this prototype.
- b. Cool down method: The device is permitted to cool for a period of time, during which the energy lost can be calculated based on the observed decrease in temperature. Although some data were recorded while the tank was cooling down, this information is not within the set of tests considered in this work.
- c. Comparison method: It involves having two charging/discharging processes with different idle periods before each charging process. Since all charging processes here considered start from nearly ambient conditions, thermal losses are negligible, as can be seen at the end of each discharging temperature profile, so this method cannot be applied in this study.
- d. Energy balance method: It compares the inlet and the outlet enthalpies after stabilization or stationary conditions. This is the method used in this work. The thermal loss power is calculated according to:

$$P_{loss} = (\dot{m}c_p)_{HTF}(T_{in} - T_{out})_{ss}$$

The representative figures during the discharging processes show that there is no temperature difference between the inlet and the outlet HTF when steady-state temperature is reached (see Appendix A). This is not the case in charging processes (see Appendix B), where there is a clear difference between inlet and outlet conditions: the abovementioned asymptotic value of temperature difference is shown in Table 5. This temperature difference permits the calculation of thermal losses by,

$$P_{loss} = (\dot{m}c_p)_{HTF}(T_{in} - T_{out})_{ss.ch}$$

Fig. 10 (a) shows the variation of the thermal losses versus different reference temperatures for each charging test: the maximum inlet air temperature, $T_{in,max}$, the maximum packed-bed temperature, $T_{pb,max}$, the mean packed-bed temperature at stationary conditions, $T_{pb,ss}$, and the temperature difference between the packed-bed at steady-state and

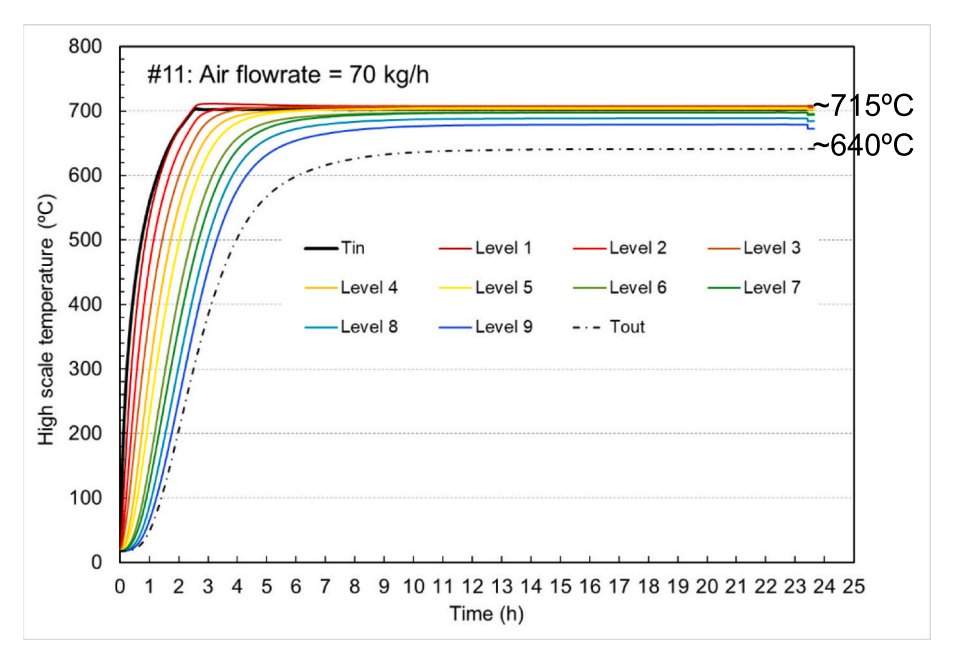


Fig. 7. Charging process #11.

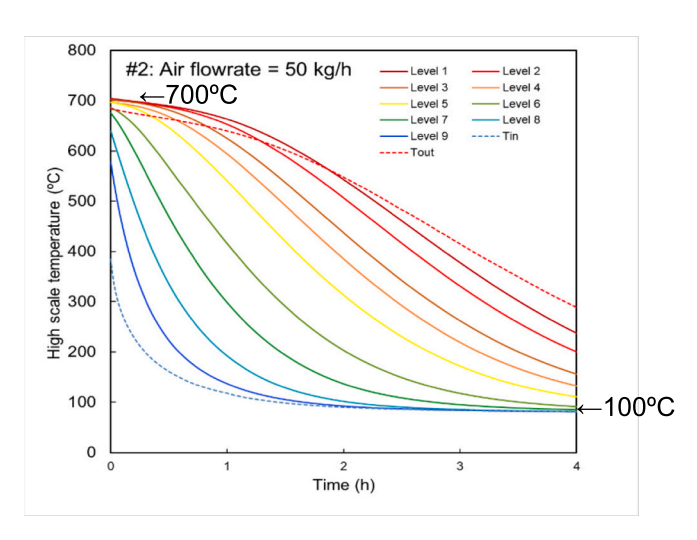


Fig. 8. Detailed temperature profile in test #2.

Table 9 Theoretical Storage Capacities, assuming a $(mc_p)_{ALTAYR}=3,75\cdot10^5~\mathrm{J/K}.$

	Charg	Charge		arge			
Air mass flow (kg/s)		T _{in,rated} (°C)		T _{out,rated} (°C)	TSC (J)	TSC (kWh)	
50	#1	710	#2	700	1,34·10 ⁸	37,3	
50	#3	760	#4	750	$1,47 \cdot 10^{8}$	40,9	
50	#5	810	#6	800	$1,57 \cdot 10^{8}$	43,7	
50	#7	855	#8	850	$1,65 \cdot 10^{8}$	45,9	
60	#9	715	#10	700	$1,41 \cdot 10^{8}$	39,1	
70	#11	715	#12	700	$1,43 \cdot 10^8$	39,8	

ambient, $(T_{pb,ss}$ - $T_{amb})$. In all the above cases, the HTF heat capacity is based on the mean value of the temperature between the inlet and outlet at steady-state conditions. Fig. 10 (b) presents, for a mass flow of 50 kg/h, the variation of the thermal losses with the mean packed-bed temperature minus ambient temperature at steady-state.

If a heat loss coefficient wants to be given, it should be related to the temperature difference between the storage device (mean temperature of the storage material) and the ambient temperature at steady-state, $(T_{pb,ss}-T_{amb})$. This heat loss coefficient multiplied by the exchange area, $A \cdot h$, is the slope of the linear fit of the different values obtained for the same mass flow rate (Fig. 10 (b)). Such a slope gives a value of 3,15 W/K for 50 kg/h air mass flow. The fit does not include a constant equal to zero, because it can (and it does) happen that, due to the insulation of the tank, the thermal losses become negligible when the packed-bed is still warm. According to the obtained fit, this happens when the mean temperature of the packed-bed is around 240 °C. Fig. 10 (b) also includes the linear fit including a constant equal to zero (green dashed line) for comparison with the usual expression (orange continuous line).

Storage Efficiency, η_{TES} , compares the energy gained by the HTF from the storage device during discharge, E_d , and the energy given by the HTF during charge, E_{ch} , being charge and discharge consecutive processes. It follows the next expression,

$$\eta_{TES} = \frac{E_d}{E_{ch}} = \frac{SC}{E_{ch}}$$

 E_{ch} is calculated assuming a charging time defined at which the air temperature difference between its inlet and outlet reaches the asymptotic temperature value plus 5 °C,

$$E_{ch} = \Delta t \frac{1}{2} \sum_{i=2}^{n_{ch}} (P_i + P_{i-1}) \text{ with } P_i = \dot{m_i} \int_{T_{curi}}^{T_{in,i}} c_{p_{HTF}}(T) dT.$$

As an example, Fig. 11 depicts a complete cycle with of one charge and a consecutive discharge, which are required to evaluate the Storage Efficiency. It can be seen the 92 °C difference between the HTF inlet and outlet difference at steady-state in charge. This temperature difference reveals the thermal losses the prototype has and the non-negligible difference between the HTF outlet temperature and the temperature at lowest part of the packed-bed (Level 9, in blue). In this figure, the different approaches to follow for the discharging times, $t_{\rm dis}$, are shown

Table 10 shows the Storage Efficiencies using different discharging time criteria. The behaviour of the Storage Efficiency in relation to the definition of the discharging time can be seen in Fig. 12. There, and as expected, it is clear that defining the end of discharge when the 70 % of the inlet temperature/enthalpy is obtained at the output implies much lower storage efficiencies, i.e., the energy provided to the TES device is much less well-used.

The general behaviour of the Storage Efficiency in relation to

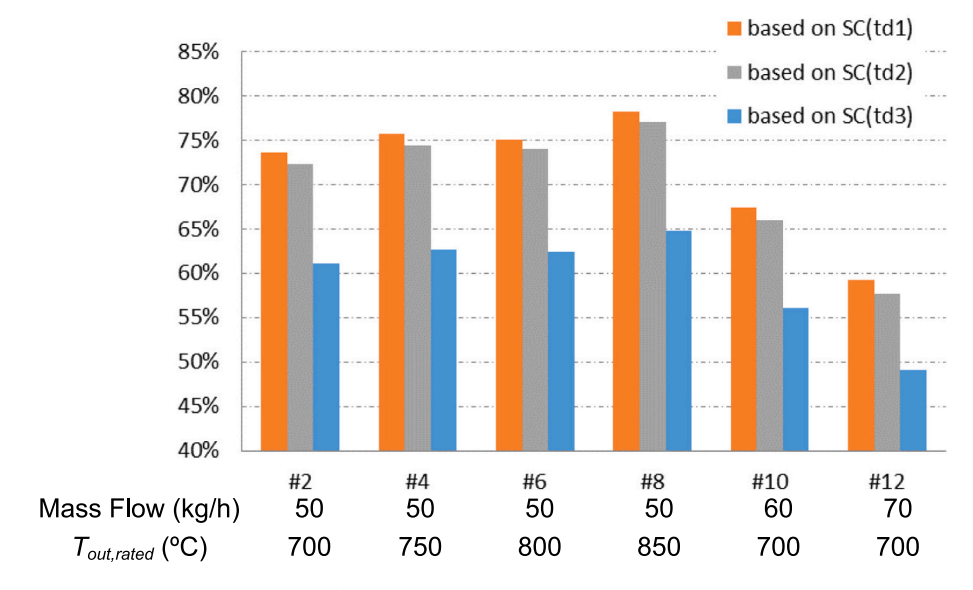


Fig. 9. Utilization Rate for different discharging processes.

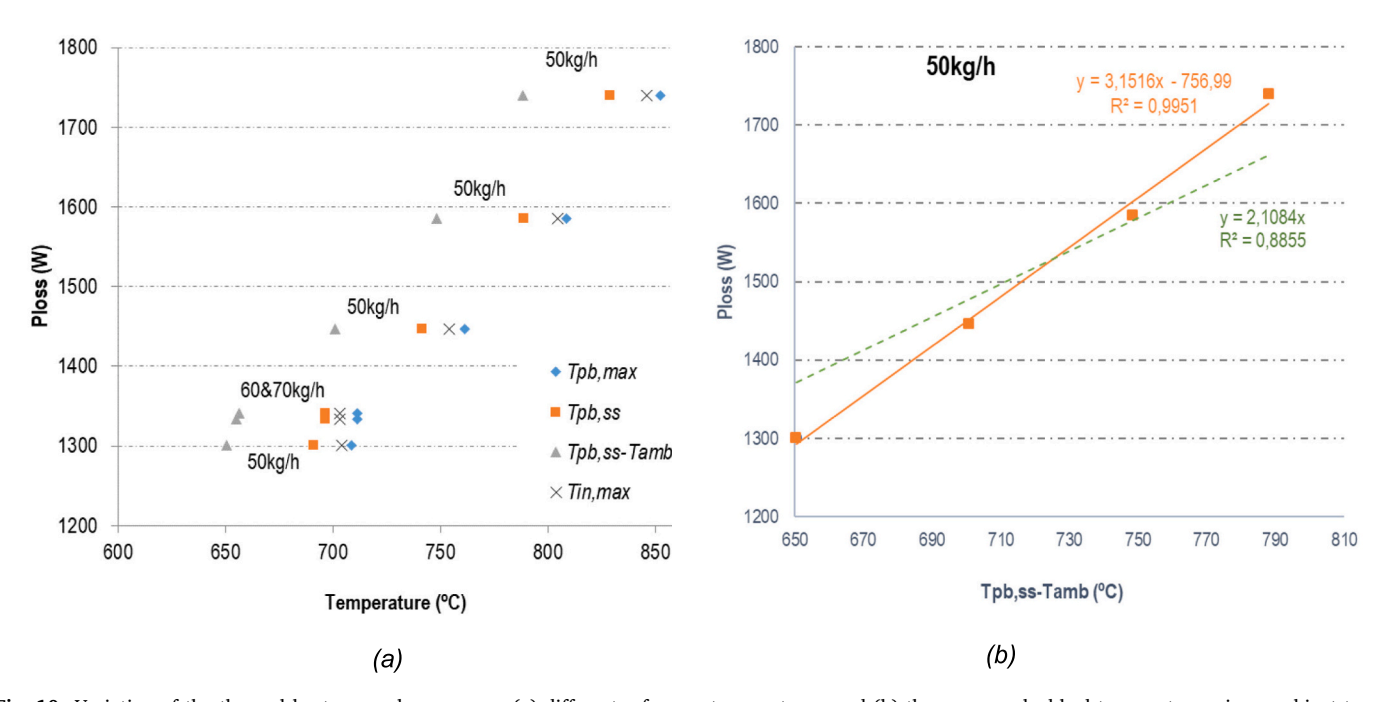


Fig. 10. Variation of the thermal heat power losses versus (a) different reference temperatures, and (b) the mean packed-bed temperature minus ambient temperature at charging steady-state conditions for a mass flow of 50 kg/h.

different rated temperatures and mass flows is similar independently of the criterion used for defining the discharging time. Since the discharging time t_{d3} is defined from having a stored energy of 70 % of the gained one, the storage efficiency is much lower than those obtained from temperature difference of 5 °C in the HTF (t_{d1}) or in the top and bottom levels of the packed-bed (t_{d2}). Interesting to mention than the highest storage efficiency is at the highest air mass flow, and it is below 75 %.

Storage exergy efficiency, ψ_{TES} , compares the exergy provided by, Ξ_{ch} , and released to, Ξ_{d} , the heat transfer fluid during consecutive charging and discharging processes, following a similar approach for the storage energy efficiency,

$$\psi_{TES} = \frac{\Xi_d}{\Xi_{ch}}$$

According to Rosen [58], the exergy, Ξ , for each process can be expressed by,

$$\mathcal{Z} = \int igg(1 - rac{T_{amb}}{T}igg) dE$$

Where T_{amb} is the ambient temperature, E the energy provided by, in charge, and to, in discharge, and T is the inlet HTF temperature in charge and the outlet HTF temperature in discharge. Several assumptions are made with this approach: nearly constant ambient temperature, negligible pressure drop and chemical, kinetic and potential energies [48]. Specifically, exergy for each process has been calculated according to:

$$egin{aligned} egin{aligned} egin{aligned} egin{aligned} egin{aligned} egin{aligned} E_{ch} = \sum_{i=2}^{n_{ch}} \left(1 - rac{T_{amb,i} + T_{amb,i-1}}{T_{in,i} + T_{in,i-1}}
ight) (P_i - P_{i-1}) \Delta t \end{aligned}$$

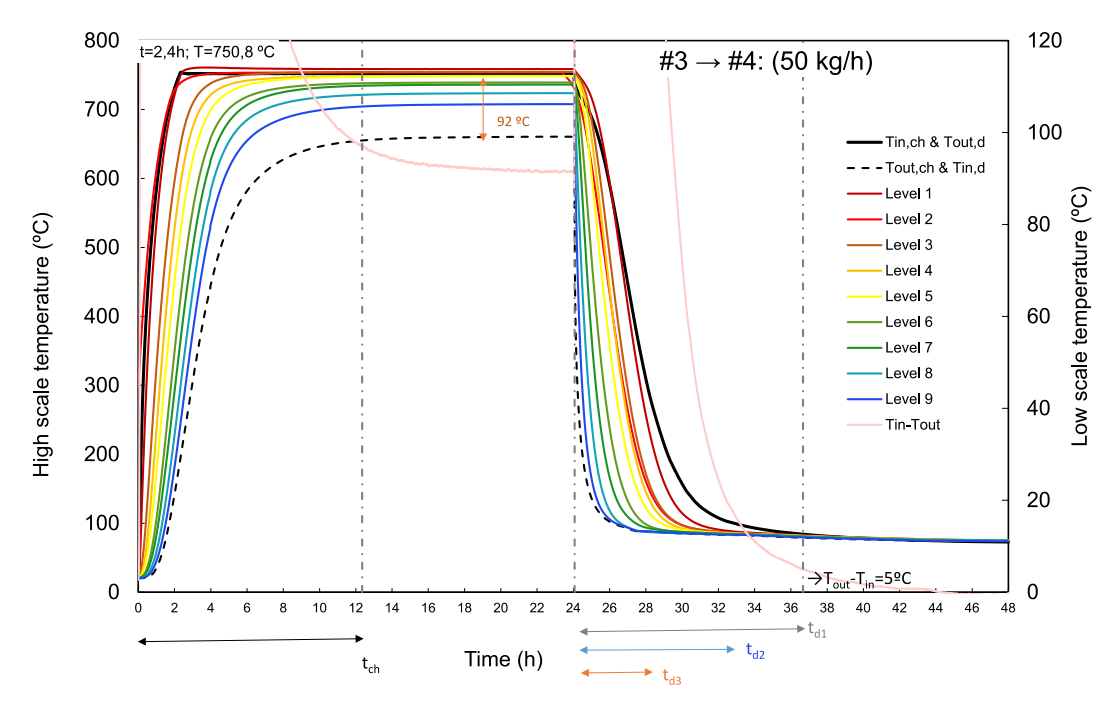


Fig. 11. Consecutive charge and discharge. Low scale axis only for T_{in} - T_{out} -

Table 10
Storage Efficiency using the charging times of Table 6.

Air mass flow (kg/h)	Charge	Disch.	$\eta_{TES}(t_{d1})$	$\eta_{TES}(t_{d2})$	$\eta_{TES}(t_{d3})$
50	#1	#2	70,1 %	68,9 %	58,2 %
50	#3	#4	66,6 %	65,5 %	55,1 %
50	#5	#6	66,0 %	65,1 %	55,0 %
50	#7	#8	63,1 %	62,2 %	52,2 %
60	#9	#10	69,9 %	68,3 %	58,1 %
70	#11	#12	72,1 %	70,1 %	59,8 %

$$\boldsymbol{\mathcal{Z}}_{d} = \sum_{i=2}^{n_{d}} \bigg(1 - \frac{T_{amb,i} + T_{amb,i-1}}{T_{out,i} + T_{out,i-1}}\bigg) (P_{i} - P_{i-1}) \Delta t$$

In Table 11 the obtained figures for the exergy and the related efficiency are shown. For their calculation the discharging time, t_{dI} , i.e., the one based on achieving a 5 °C temperature difference between the air inlet and outlet, is used. The so obtained exergy efficiencies are lower than the corresponding energy efficiency values in Table 10, reflecting that the usefulness of thermal energy given at a practical temperature is lower than an equal quantity of any work-equivalent energy form. As expected, and since exergy considers the temperature level and the transferred energy, for the same air mass flow, the higher the rated temperature, the higher the exergy and for the same rated temperature, the lower the air mass flow the higher exergy. It is interesting to mention

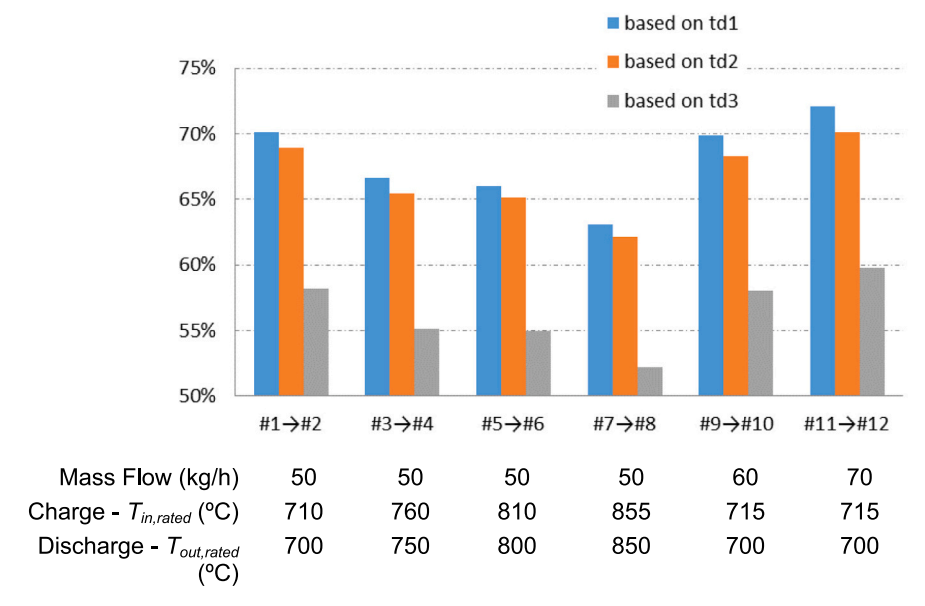


Fig. 12. Storage Efficiencies according to data on Table 10.

Storage media

Table 11 Exergy, \mathcal{Z} , values in consecutive charge and discharge and the corresponding Storage Exergy Efficiency, Ψ_{TES} .

	Charg	e		Disch	Discharge				
Air mass flow (kg/s)		T _{in,rated} (°C)	Ξ _{ch} (kWh)		T _{out,} rated (°C)	Ξ_d (kWh)	Ψ_{TES}		
50	#1	710	39,59	#2	700	26,31	66 %		
50	#3	760	44,00	#4	750	27,45	62 %		
50	#5	810	47,09	#6	800	29,37	62 %		
50	#7	855	53,89	#8	850	32,56	60 %		
60	#9	715	33,98	#10	700	22,52	66 %		
70	#11	715	30,47	#12	700	20,58	68 %		

that the behaviour of the Exergy Efficiency has the same tendency as the Utilization Rate. It is also interesting to see when comparing the energy and exergy efficiencies that the last ones are 90–95 % of the former ones, which is quite high due to the temperatures we are working with.

The last KPI SFERA-III proposes is the **Auxiliary power consumption**, or parasitic power consumption. It is the electric consumption of any auxiliary device needed to operate the TES prototype. In the prototype here studied, it would refer to the consumption of the compressor. Unfortunately, there is not a specific power meter for that, so it is not possible to evaluate that KPI.

As suggested in SFERA-III procedures, a final evaluation table should be included in any study dealing with the assessment of the thermal performance of any TES prototype. In the case of the packed-bed here studied, it corresponds to Table 12.

6. Conclusions

The key performance indicators, KPIs, of a packed-bed prototype have been evaluated in accordance with the procedures and definitions established in the guideline proposed in the SFERA-III project with the aim of increasing the variety of TES prototypes tested under such approach. The packed-bed prototype under examination is installed in the ALTAYR facility which comprises a 0,1 $\rm m^3$ tank with Rethink Seramic Flora® as solid filler and atmospheric air as HTF. Tests were conducted under a variety of operational conditions, with discharging outlet temperatures ranging from 700 $^{\circ}{\rm C}$ to 850 $^{\circ}{\rm C}$ and air mass flows between 50 kg/h to 70 kg/h.

- The KPIs obtained are as follows: Discharging Time, Storage Capacity, Mean Thermal Power, Utilization Rate, Thermal Losses (dynamic), Storage (energy) Efficiency and Storage Exergy Efficiency.
- As SFERA-III KPIs are primarily calculated using HTF temperature at both prototype inlet and outlet, it is of paramount importance to have accurate measurements of these variables in appropriate locations, free from the influence of thermal bridges that could otherwise confound the readings.
- It has been observed that the criterion used to define discharging time becomes decisive to obtaining the rest of KPIs. Consequently, a number of approaches have been analysed, including HTF temperature difference between tank inlet and outlet at 5 °C or 3 °C, HTF output enthalpy 70 % inlet enthalpy and even using the top and bottom temperature difference within the packed-bed at 5 °C.
- \bullet Assuming that discharging process ends when HTF temperature difference between tank inlet and outlet is 5 °C, the Storage Capacities obtained are between 23 and 36 kWh, the Utilization Rates between 55 %–80 %, Storage Efficiencies between 63 % to more than 70 %, and Exergy Efficiencies between 60 % and 68 %. The slight

Table 12General information of the state and conditions while evaluating the packed-bed prototype here studied.

Storage geometry		
Tank geometry	Cylinder Packed-bed with empty volumes at the top and at the bottom of the bed. 0,1	
Tank boundaries		
Tank volume (m³)		
Material properti	es	
	Type	Air
HTF	Specific heat (J/(kg.K))	$0,2 \cdot T(^{\circ}C) + 990$
	Total volume (m ³)	0,05
Ct1:-	Specific heat (J/(kg.K))	1024
	Density (kg/m ³)	2700

 ~ 130

Rethink Seramic Flora®

Total mass (kg)

Type

	Туре	Retillik Serailic Floras	
Operating Condit	ions		
Initial conditions		Discharge: steady-state full charge state Charge: steady-state condition	
Ambient temperature		38 °C (mean value)	
Start of charge criterion		Electric heaters on	
End of charge criterion		$(T_{in}-T_{out}) \leq 5^{\circ}C$	
Start of discharge criterion		Electric heaters off	
End of discharge criterion		$(T_{out} - T_{in}) \leq 5^{\circ} C$	
Test Conditions	HTF flow rate charge and	$\dot{m} \in \{50, 60, 70\} \text{ kg/h}$	
	discharge		
	Inlet/Outlet rated temperatures (°C)		
	Charge:	710/610–715/630–715/640–760/ 660–810/700–855/735	
	Discharge:	100/700-100/750-100/800-100/850	
Thermal losses	Can be estimated from this dataset?	Yes	
	If Yes, method used*	Energy Balance Method at constant temperature and flow rate (dynamic heat losses)	
Auxiliary power consumption	Do we monitor this?	No	

difference between these two efficiencies can be attributed to the high temperatures at which the TES prototype operates.

The analysis demonstrates that the SFERA-III Key Performance Indicators (KPIs) are an appropriate means of evaluating packed bed thermal energy storage prototypes. Consequently, the use of these KPIs as a standard is supported.

CRediT authorship contribution statement

Esther Rojas: Writing – original draft, Project administration, Methodology, Formal analysis, Data curation, Conceptualization. Elisa Alonso: Writing – review & editing, Investigation, Data curation. Margarita Rodríguez-García: Writing – review & editing, Investigation. Rocío Bayón: Writing – review & editing, Investigation. Antonio Avila-Marín: Writing – review & editing, Investigation, Data curation.

Declaration of competing interest

The authors declare that they have not known competing financial interest or personal relationships that could have appeared to influence the work reported in this paper

Data availability

Acknowledgements

Data will be made available on request.

This work has been supported by the European Union's Horizon H2020 Research and Innovation Programme through SFERA III Project (GA.823802)

Appendix A. Temperature profiles for the discharging tests

Appendix A presents the detail information for all the discharging tests except test #2, which is described in section 4.1 (Fig. 5). Fig. A.1 to Fig. A.5 show the evolution of the air with the time through the packed bed at different levels for the discharging test #4, #6, #8, #10 and #12. The air mass flow rate and the approximate initial air temperature are shown in Table 4. Some of the main parameters and the related KPIs of all these tests are thoroughly discussed in section 3 and section 4 respectively.

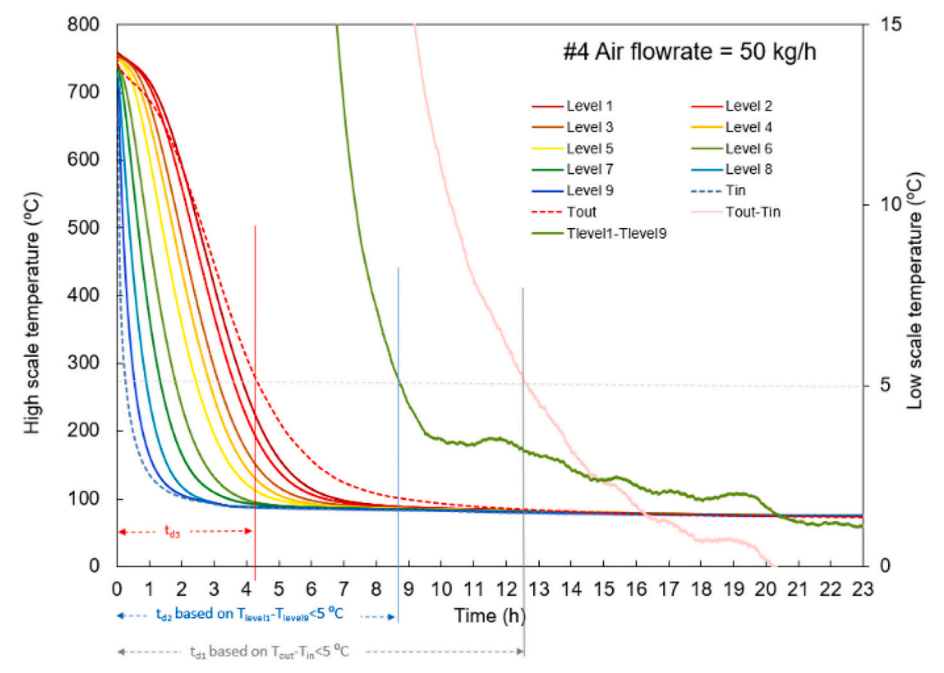


Fig. A.1. Discharge #4. Low temperature scale for temperature differences (T_{in} - T_{out}) and (T_{level1} - T_{level9}).

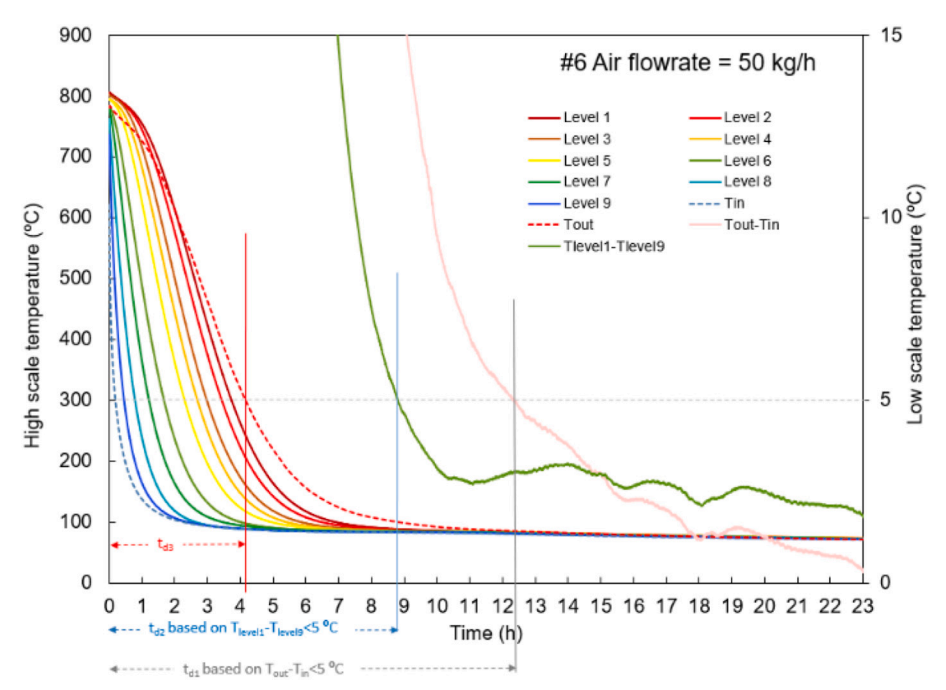


Fig. A.2. Discharge #6. Low temperature scale for temperature differences (T_{in} - T_{out}) and (T_{level1} - T_{level9}).

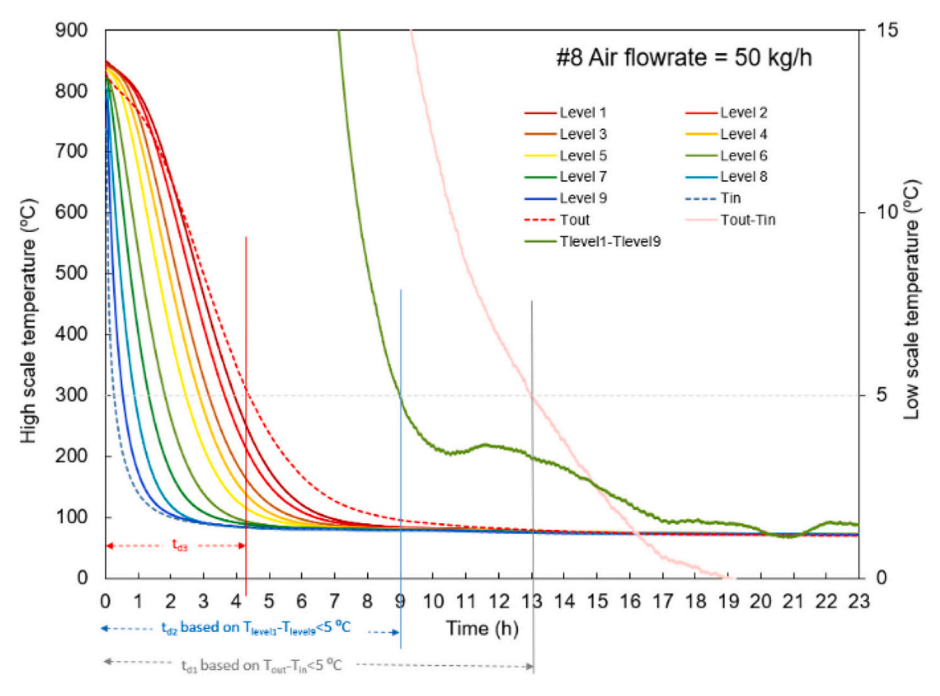


Fig. A.3. Discharge #8. Low temperature scale for temperature differences (T_{in} - T_{out}) and (T_{level1} - T_{level9}).

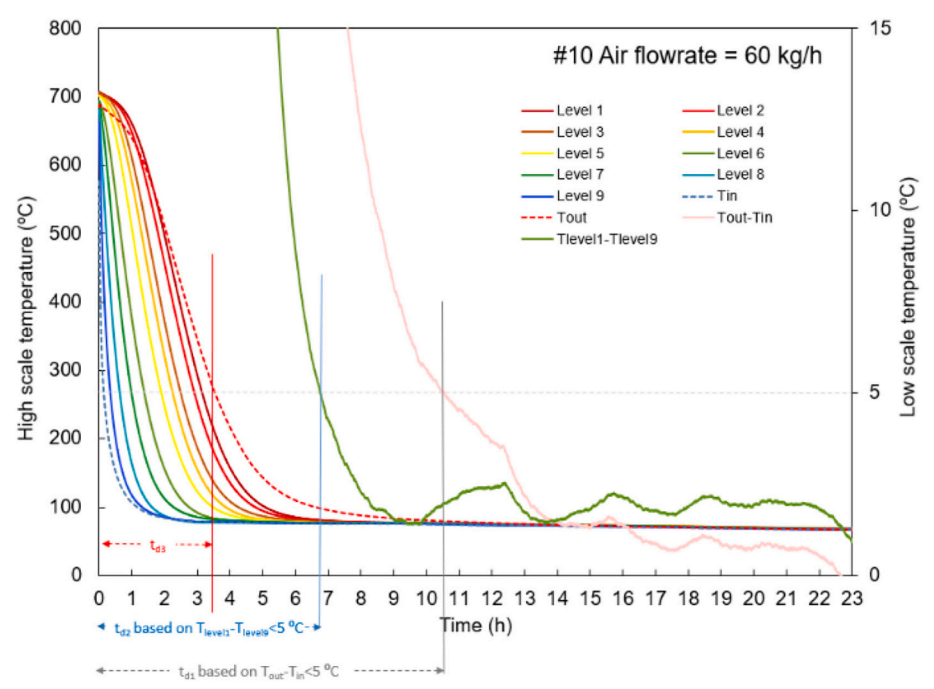


Fig. A.4. Discharge #10. Low temperature scale for temperature differences (T_{in} - T_{out}) and (T_{level1} - T_{level9}).

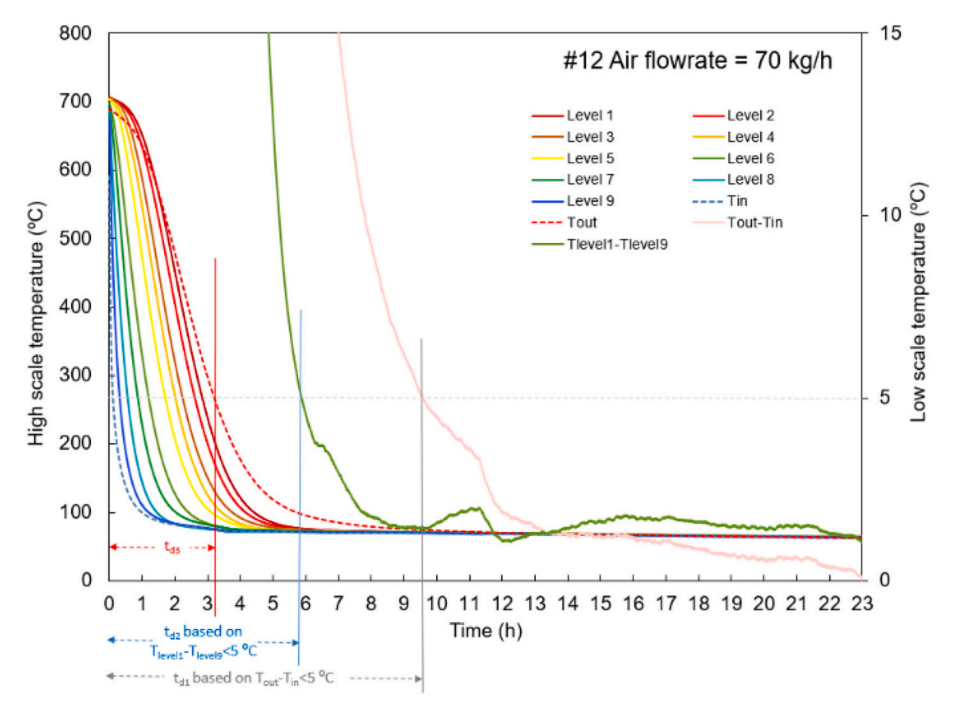


Fig. A.5. Discharge #12. Low temperature scale for temperature differences $(T_{in}-T_{out})$ and $(T_{levell}-T_{level9})$.

Appendix B. Temperature profiles for the charging tests

Appendix B presents the detail information for all the charging tests except test #1, which is presented in section 4.2 (Fig. 6). Fig. B.1 to Fig. B.5 show the evolution of the air with the time through the packed bed at different levels the charging process test #3, #5, #7, #9 and #11. The air mass flow rate and the approximate initial air temperature are shown in Table 6. Some of the main parameters and the related KPIs of all these tests are thoroughly discussed in section 3 and section 4 respectively.

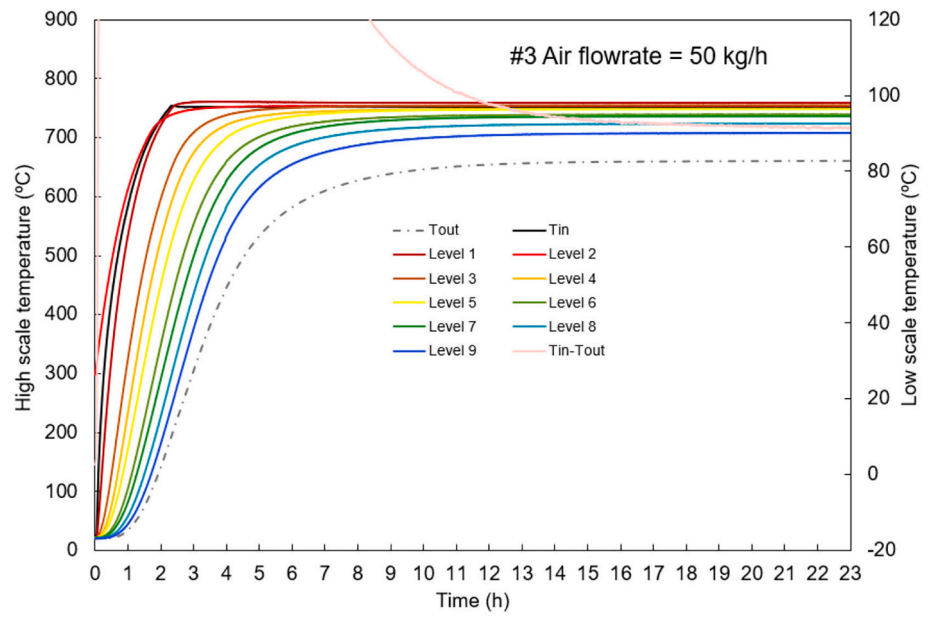
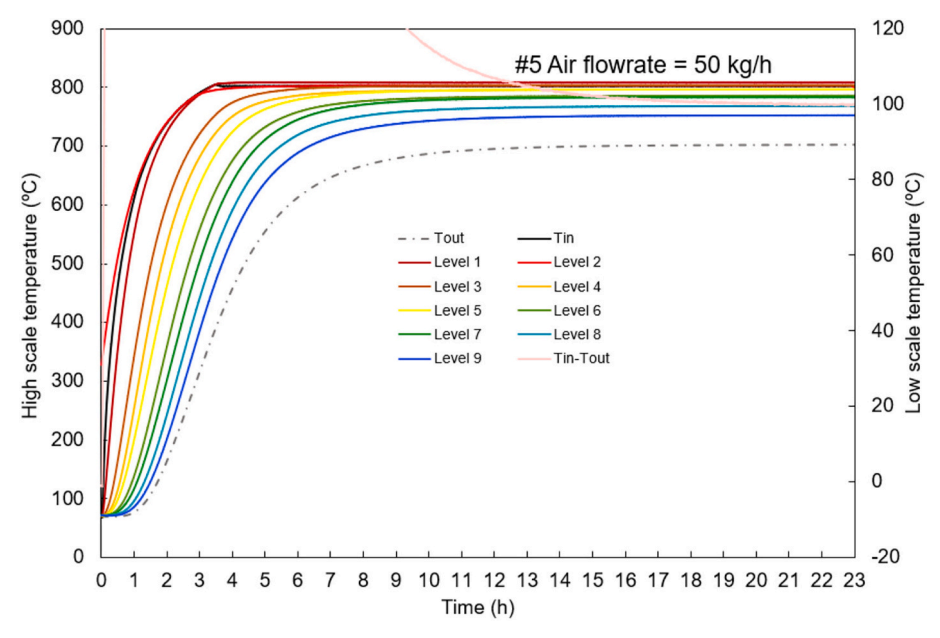


Fig. B.1. Charge #3. Low temperature scale for temperature differences (T_{in} - T_{out}) and (T_{level1} - T_{level9}).



 $\textbf{Fig. B.2.} \ \ \text{Charge \#5. Low temperature scale for temperature differences } (\textit{T}_{\textit{in-}}\textit{T}_{\textit{out}}) \ \ \text{and} \ \ (\textit{T}_{\textit{level1-}}\textit{T}_{\textit{level9}}).$

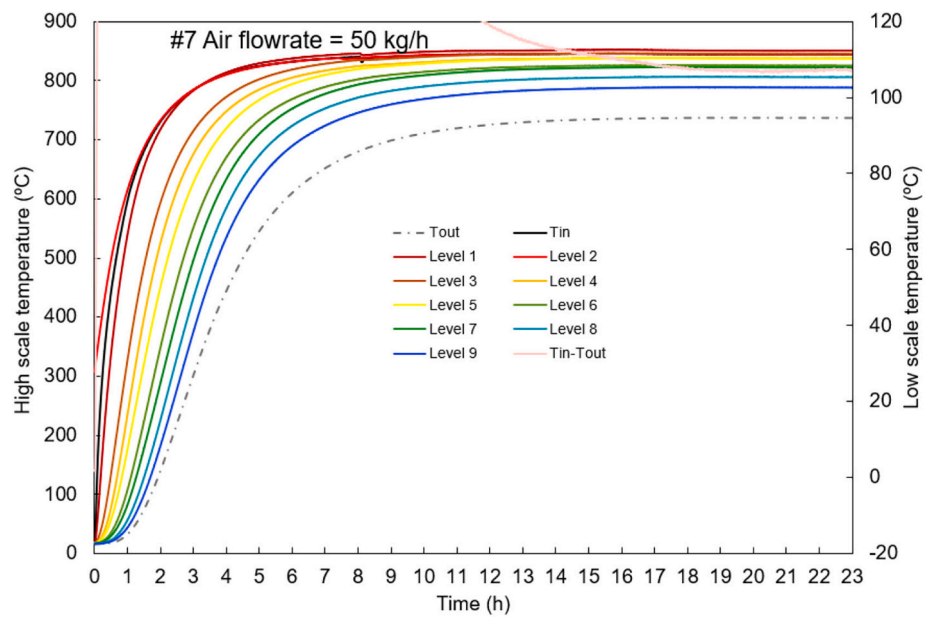


Fig. B.3. Charge #7. Low temperature scale for temperature differences (T_{in} - T_{out}) and (T_{level1} - T_{level9}).

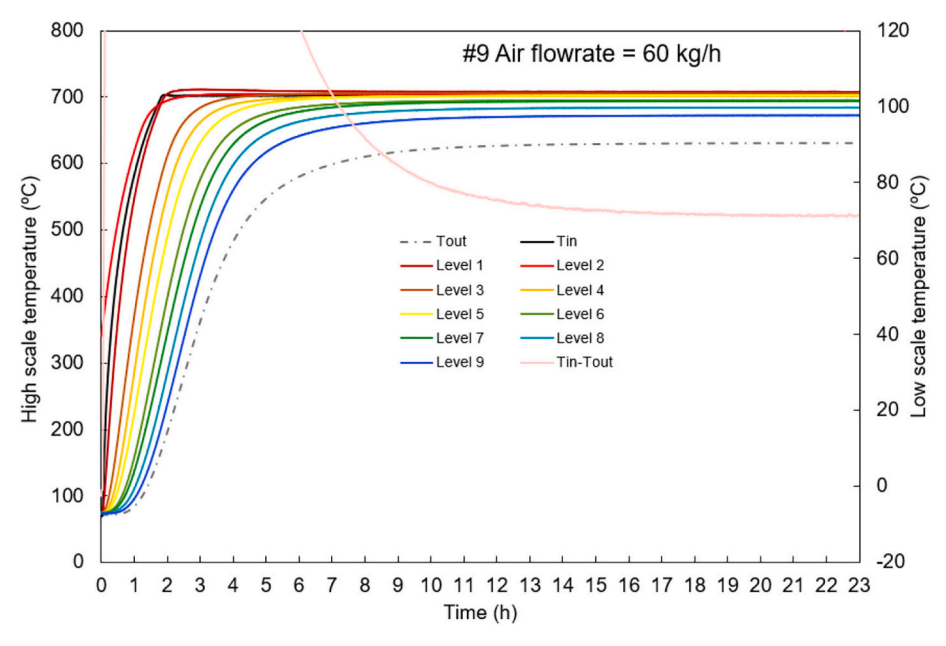


Fig. B.4. Charge #9. Low temperature scale for temperature differences (T_{in} - T_{out}) and (T_{level} - T_{level} - T_{level}).

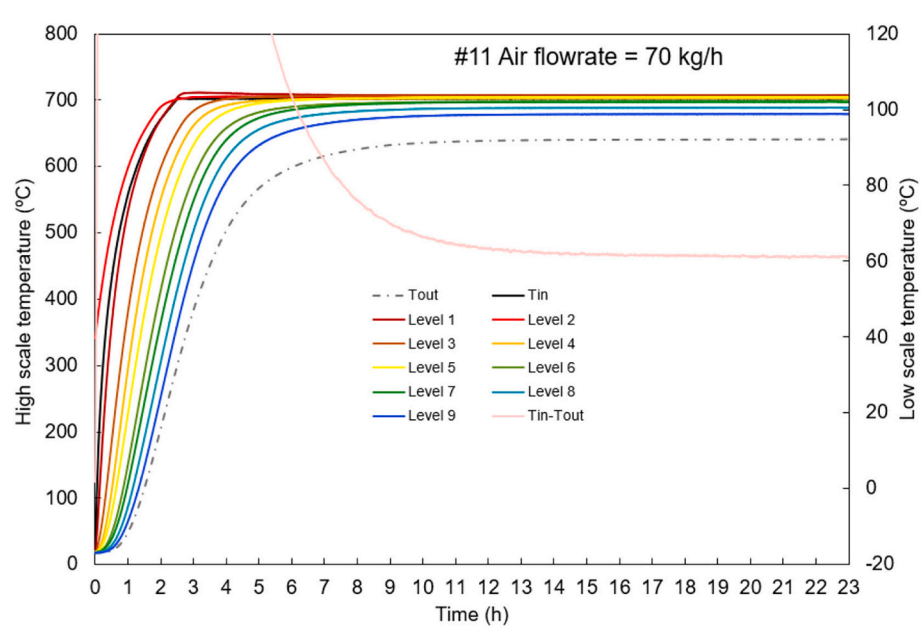


Fig. B.5. Charge #11. Low temperature scale for temperature differences (T_{in} - T_{out}) and (T_{level1} - T_{level9}).

References

- EASE/EERA, "Joint EASE/EERA recommendations for a European Energy Storage Technology Development Roadmap. 2017 Update", https://www.eera-set.eu/component/attachments/?task=download&id=312.
- [2] SENER, "Planta termosolar CCP NOOR Ouarzate II". Accessed: Sep. 28, 2023. [Online]. Available, https://www.group.sener/proyecto/planta-termosolar-cc
- [3] SENER, "Planta termosolar de torre central NOOR III, en Ouarzazate (Marruecos)". Accessed: Sep. 28, 2023. [Online]. Available, https://www.group. sener/proyecto/termosolar-torre-nooro-iii-ouarzazate/#.
- [4] Atlantica Sustainable Infrastructure plc, "Solana". Accessed: Sep. 28, 2023.
 [Online]. Available, https://www.atlantica.com/web/en/company-overview/our-assets/asset/Solana/
- [5] Crespo L. "The double role of CSP plants on the future electrical systems", WBG Conference 'Concentrating Solar for Power and Heat. Apr. 2020.
- [6] Schöniger F, Thonig R, Resch G, Lilliestam J. Making the sun shine at night: comparing the cost of dispatchable concentrating solar power and photovoltaics

- with storage. Energy Sources B: Econ Plan Policy Jan. 2021;16(1):55–74. https://doi.org/10.1080/15567249.2020.1843565.
- [7] En IR, Irena A. Innovation outlook: Thermal energy storage. Abu Dhabig; 2020.
- [8] Schumacher M. "ETES: Electric Thermal Energy Storage. How thermal power plants can benefit from the energy transition," in The Future of Energy 2019, 2019. Accessed: Sep. 28, 2023. [Online]. Available, https://assets.new.siemens.com/siemens/assets/api/uuid:6f83e987-b0b8-4663-8a19-cd011682f9a0/3-schumacher-benefits-of-energy-transition-for-thermal-power-pla.pdf.
- [9] Tani S. "New energy storage technologies hold key to renewable transition". Special report The future of Energy. Finantial Times Nov. 2022. Accessed: Sep. 28, 2023. [Online]. Available: https://www.ft.com/content/4c8919a3-5d94-4772-9aa 2-3d6186170009.
- [10] Rayner T. Innovations in long-duration energy storage. PV Magazine USA 2/2023. Accessed: Oct. 03, 2023. [Online]. Available: https://pv-magazine-usa.com/2023/02/20/innovations-in-long-duration-energy-storage/.
- [11] Kauko H, et al. "Industrial Thermal Energy Storage. Supporting the transition to decarbonise industry", Dec. 2022. Accessed: Sep. 28, 2023. [Online]. Available, htt ps://www.eera-eeip.eu/news-and-resources/3867-thermal-energy-storage-couldsave-the-eu-over-500mt-co2-per-year-34.html.

- [12] ANSI/ASHRAE. "Methods of Testing Active Sensible Thermal Energy Devices Based on Thermal Performance", ANSI/ASHRAE Standards 94.3–2010. 2010.
- [13] ANSI/ASHRAE. "Methods of Testing Active Latent –Heat Storage Devices Based on Thermal Performance", ANSI/ASHRAE Standards 94.1–2010. 2010.
- [14] Müller-Trefzer F, Niedermeier K, Daubner M, Wetzel T. Experimental investigations on the design of a dual-media thermal energy storage with liquid metal. Appl Therm Eng 2022;213:118619. https://doi.org/10.1016/j. applthermaleng.2022.118619.
- [15] Seubert B, Müller R, Willert D, Fluri T. Experimental results from a laboratory-scale molten salt thermocline storage. AIP Conf Proc Jun. 2017;1850(1):080025. https://doi.org/10.1063/1.4984446.
- [16] SFERA Project (GA. 228296), "SFERA Solar Facilities for the European Research Area. Project Final Report", 2014. Accessed: Oct. 04, 2023. [Online]. Available, htt ps://cordis.europa.eu/project/id/228296/reporting.
- [17] Rojas E, Bayón R. "Definition of standardised procedures for testing thermal storage prototypes for concentrating solar thermal plants," 2011. Accessed: Oct. 04, 2023. [Online]. Available, https://sfera.sollab.eu/index.php?page=j oint wp15.
- [18] Rojas E., "Thermal energy storage working group", SolarPACES TCP. Accessed: Oct. 04, 2023. [Online]. Available, https://www.solarpaces.org/csp-research-tasks/task-iii-solar-technology-and-advanced-applications/thermal-energy-storage-working-group/.
- [19] UNE, "Caracterización del sistema de almacenamiento térmico para aplicaciones de concentración solar con captadores cilindroparabólicos", UNE 206012:2017. 2017. Accessed: Oct. 04, 2023. [Online]. Available, https://www.une.org/encuentra-tu-norma/busca-tu-norma/orma?c=N0058279.
- [20] TC/SC 117, "Solar thermal electric plant Part 2–1: Thermal energy storage systems –characterization of active, sensible systems for direct and indirect configurations", IEC TS 62862–2-1:2021. 2021. Accessed: Oct. 04, 2023. [Online]. Available, https://webstore.iec.ch/publication/31588.
- [21] Romani J, Gasia J, Cabeza LF. "Definitions of technical parameters for thermal energy storage (TES)," Available on line from International Energy Agency, ECES, Annex 30: Thermal Energy Storage for cost effective energy management & CO2 mitigation, https://www.eces-a30.org/; 2018.
- [22] SFERA-III web page. Accessed: Oct 2023;04 [Online]. Available: https://sfera3.sollab.eu/about-us/.
- [23] Azevedo P, et al. "D6.3: Protocol for testing sensible and latent storage prototypes Towards the Standardization of testing prototypes for storage systems," 2023. Available, https://sfera3.sollab.eu/wp-content/uploads/2023/12/SFERA-III-D6.3-Protocol-for-testing-sensible-and-latent-storage-prototypes.pdf.
- [24] García P. "Case studies on latent heat storage," in IRES 2022 Workshop Towards a fair evaluation of Thermal Energy Storage prototypes - Guidelines for CSP applications, Sep. 2022. Accessed: Oct. 04, 2023. [Online]. Available, https://sfe ra3.sollab.eu/wp-content/uploads/2023/01/Pierre-Garcia-IRES-Conference-SFE RA-III-LHTES-performance-assessment red.pdf.
- [25] Liberatore R. "Case studies on thermal losses calculations," in IRES 2022 -Workshop Towards a fair evaluation of Thermal Energy Storage prototypes – Guidelines for CSP applications, Sep. 2022. Accessed: Oct. 04, 2023. [Online]. Available, https://sfera3.sollab.eu/wp-content/uploads/2022/12/Raffaele-Libera tore-SFERA-III_IRES-Presentation_Thermal-losses_220921_compressed.pdf.
- [26] Weiss J. "Case studies on sensible heat storage," in IRES 2022 Workshop Towards a fair evaluation of Thermal Energy Storage prototypes – Guidelines for CSP applications, Sep. 2022. Accessed: Oct. 04, 2023. [Online]. Available. https://sfe ra3.sollab.eu/wp-content/uploads/2022/12/Julius-Weiss-220921_SFERA-III_Wo rkshop sensible storages Weiss.pdf.
- [27] Li M-J, Jin B, Yan J-J, Ma Z, Li M-J. Numerical and experimental study on the performance of a new two-layered high-temperature packed-bed thermal energy storage system with changed-diameter macro-encapsulation capsule. Appl Therm Eng 2018;142:830–45. https://doi.org/10.1016/j.applthermaleng.2018.07.026.
- [28] Xu Y, He YL, Li YQ, Song HJ. Exergy analysis and optimization of charging-discharging processes of latent heat thermal energy storage system with three phase change materials. Sol Energy Jan. 2016;123:206–16. https://doi.org/ 10.1016/J.SOLENER.2015.09.021.
- [29] He X, Qiu J, Wang W, Hou Y, Ayyub M, Shuai Y. Optimization design and performance investigation on the cascaded packed-bed thermal energy storage system with spherical capsules. Appl Therm Eng 2023;225:120241. https://doi. org/10.1016/j.applthermaleng.2023.120241.
- [30] Xie B, Li C, Wang M, Liu C, Chen J, Orji WU. Experimental and numerical study of epoxy resin-based composite phase change material in packed-bed thermal energy storage system for ventilation. Energ Buildings 2023;291:113145. https://doi.org/ 10.1016/j.enbuild.2023.113145.
- [31] Lu S, Jia Y, Liang B, Wang R, Lin Q, He Z. Optimal design and thermal performance study of a two-stage latent heat thermal energy storage technology for heating systems. Appl Therm Eng 2023;232:121073. https://doi.org/10.1016/j. applthermaleng.2023.121073.
- [32] Shen Y, Zhang P, Rehman Mazhar A, Chen H, Liu S. Experimental analysis of a finenhanced three-tube-shell cascaded latent heat storage system. Appl Therm Eng 2022;213:118717. https://doi.org/10.1016/j.applthermaleng.2022.118717.
- [33] Fan M, et al. Charging and discharging characteristics of cascaded latent heat storage (CLHS) tank for low-temperature applications. Appl Therm Eng 2022;213: 118698. https://doi.org/10.1016/j.applthermaleng.2022.118698.
- [34] Salem MR, Owyed MN, Ali RK. Experimental investigation of the performance attributes of a thermal energy storage unit using different system configurations.

- Appl Therm Eng 2023;230:120678. https://doi.org/10.1016/j.applthermaleng.2023.120678.
- [35] Lu S, Zhai X, Gao J, Wang R. Performance optimization and experimental analysis of a novel low-temperature latent heat thermal energy storage device. Energy 2022;239:122496. https://doi.org/10.1016/j.energy.2021.122496.
- [36] Lazaro A, Delgado M, Konig-Haagen A, Hohlein S, Diarce G. "Technical performance assessment of phase change material components," in Proceedings of the ISES Solar World Conference 2019 and the IEA SHC Solar Heating And Cooling Conference for Buildings and Industry 2019, J. M. Cardemil, K. Guthrie, and R. Ruther, Eds., Wiesentalstr 50, Freiburg, 79115, Germany: Intl Solar Energy Soc. 2019. https://doi.org/10.18086/swc.2019.22.05. pp. 1206–1217.
- [37] Hauer A, et al. "TASK 58 / ANNEX 33: Material and Component Development for Thermal Energy Storage, 2020.," 2020. Accessed: Oct. 04, 2023. [Online]. Available: chrome-extension://efaidnbmnnnibpcajpcglclefindmkaj/, https://iea-es.org/wp-content/uploads/public/IEA-ES-TCP-Annex-33-Final-Report_revised-May-2021.pdf.
- [38] König-Haagen A, et al. Analysis of the discharging process of latent heat thermal energy storage units by means of normalized power parameters. J Energy Storage 2023;72:108428. https://doi.org/10.1016/j.est.2023.108428.
- [39] Soprani S, et al. Design and testing of a horizontal rock bed for high temperature thermal energy storage. Appl Energy 2019;251:113345. https://doi.org/10.1016/ j.apenergy.2019.113345.
- [40] Ortega-Fernández et al., "Experimental validation of steel slag as thermal energy storage material in a 400 kWht prototype," AIP Conf Proc, vol. 2126, no. 1, p. 200026, Jul. 2019, doi: https://doi.org/10.1063/1.5117741.
- [41] Zhou H, Lai Z, Cen K. Experimental study on energy storage performances of packed-bed with different solid materials. Energy 2022;246:123416. https://doi. org/10.1016/j.energy.2022.123416.
- [42] Trevisan S, Wang W, Guédez R, Laumert B. Laboratory prototype of an innovative radial flow packed-bed thermal energy storage. AIP Conf Proc May 2022;2445(1): 160018. https://doi.org/10.1063/5.0086004.
- [43] Trevisan S, Wang W, Guédez R, Laumert B. Experimental evaluation of an innovative radial-flow high-temperature packed-bed thermal energy storage. Appl Energy 2022;311:118672. https://doi.org/10.1016/j.apenergy.2022.118672.
- [44] Knobloch K, et al. A partially underground rock bed thermal energy storage with a novel air flow configuration. Appl Energy 2022;315:118931. https://doi.org/ 10.1016/j.apenergy.2022.118931.
- [45] Okello D, Nydal OJ, Banda EJK. Experimental investigation of thermal destratification in rock bed TES systems for high temperature applications. Energy Convers Manag 2014;86:125–31. https://doi.org/10.1016/j. enconman.2014.05.005.
- [46] Okello D, Foong CW, Nydal OJ, Banda EJK. An experimental investigation on the combined use of phase change material and rock particles for high temperature (~350 C) heat storage. Energy Convers Manag 2014;79. https://doi.org/10.1016/ i.enconman.2013.11.039.
- [47] Rao CRC, Niyas H, Muthukumar P. Performance tests on lab–scale sensible heat storage prototypes. Appl Therm Eng 2018;129:953–67. https://doi.org/10.1016/j. applthermaleng.2017.10.085.
- [48] Garcia P, Largiller G. Performances and control aspects of steam storage systems with PCM: key learnings from a pilot-scale prototype. Appl Energy 2022;325: 119817. https://doi.org/10.1016/j.apenergy.2022.119817.
- [49] Avila-Marin AL, Alvarez-Lara M, Fernandez-Reche J. A regenerative heat storage system for central receiver technology working with atmospheric air. Energy Procedia Jan. 2014;49:705–14. https://doi.org/10.1016/J.EGYPRO.2014.03.076.
- [50] Alonso E, Rojas E. Air solid packed-beds for high temperature thermal storage: practical recommendations for predicting their thermal behaviour. Appl Therm Eng 2022;202. https://doi.org/10.1016/j.applthermaleng.2021.117835.
- [51] Alonso E, Rojas E, Bayón R. Experimental and numerical study of an air solid thermocline thermal energy storage system operating at high temperature. AIP Conf Proc May 2022;2445(1):160001. https://doi.org/10.1063/5.0087655.
- [52] Alonso E, Rojas E. A simple method to determine the thermal capacity of fillers for sensible thermal storage under operating conditions. AIP Conf Proc Oct. 2023;2815 (1):160003. https://doi.org/10.1063/5.0148564.
- [53] Seramic Materials Ltd. Data Sheet ReThink Seramic Flora. Oct. 2020.
- [54] Al-Azawii MMS, Alhamdi SFH, Braun S, Hoffmann J-F, Calvet N, Anderson R. Experimental study on packed-bed thermal energy storage using recycled ceramic as filler materials. J Energy Storage 2021;44:103375. https://doi.org/10.1016/j. est.2021.103375.
- [55] Al-Azawii MMS, Alhamdi SFH, Braun S, Hoffmann J-F, Calvet N, Anderson R. Thermocline in packed-bed thermal energy storage during charge-discharge cycle using recycled ceramic materials - commercial scale designs at high temperature. J Energy Storage 2023;64:107209. https://doi.org/10.1016/j.est.2023.107209.
- [56] Ortega-Fernández I, et al. Operation strategies guideline for packed-bed thermal energy storage systems. Int J Energy Res Oct. 2019;43(12):6211–21. https://doi. org/10.1002/er.4291.
- [57] Biencinto M, Bayón R, Rojas E, González L. Simulation and assessment of operation strategies for solar thermal power plants with a thermocline storage tank. Sol Energy May 2014;103:456–72. https://doi.org/10.1016/J.SOLENER.2014.02.037.
- [58] Rosen MA. Appropriate thermodynamic performance measures for closed Systems for Thermal Energy Storage. J Sol Energy Eng May 1992;114(2):100–5. https:// doi.org/10.1115/1.2929986.